AD-A043 581 ARMY MISSILE RESEARCH AND DEVELOPMENT COMMAND REDSTO--ETC F/G 17/9
MILLIMETER AND SUBMILLIMETER WAVE RECEIVERS.(U)
JUL 77 J WALDMAN

UNCLASSIFIED DRDMI-TE-77-17 NL

1 OF 1
AD A043581

END
DATE FILMED
9 -77
DDC

(12)
NW

TECHNICAL REPORT TE-77-17

MILLIMETER AND SUBMILLIMETER WAVE RECEIVERS

Advanced Sensors Directorate
Technology Laboratory

14 July 1977

U.S. ARMY MISSILE RESEARCH AND DEVELOPMENT COMMAND

Redstone Arsenal, Alabama 35809

DISPOSITION INSTRUCTIONS

DESTROY THIS REPORT WHEN IT IS NO LONGER NEEDED. DO NOT RETURN IT TO THE ORIGINATOR.

DISCLAIMER

THE FINDINGS IN THIS REPORT ARE NOT TO BE CONSTRUED AS AN OFFICIAL DEPARTMENT OF THE ARMY POSITION UNLESS SO DESIGNATED BY OTHER AUTHORIZED DOCUMENTS.

TRADE NAMES

USE OF TRADE NAMES OR MANUFACTURERS IN THIS REPORT DOES NOT CONSTITUTE AN OFFICIAL INDORSEMENT OR APPROVAL OF THE USE OF SUCH COMMERCIAL HARDWARE OR SOFTWARE.

UNCLASSIFIED

SECURITY CLASSIFICATION OF THIS PAGE (When Data Entered)

REPORT DOCUMENTATION PAGE

READ INSTRUCTIONS BEFORE COMPLETING FORM

1. REPORT NUMBER: DRDMI-TE-77-17	2. GOVT ACCESSION NO.
3. RECIPIENT'S CATALOG NUMBER	
4. TITLE (and Subtitle): MILLIMETER AND SUBMILLIMETER WAVE RECEIVERS	5. TYPE OF REPORT & PERIOD COVERED: Technical Report
	6. PERFORMING ORG. REPORT NUMBER: TE-77-17
7. AUTHOR(s): Jerry Waldman	8. CONTRACT OR GRANT NUMBER(s)
9. PERFORMING ORGANIZATION NAME AND ADDRESS: Commander, US Army Missile Command, Attn: DRDMI-TE, Redstone Arsenal, Alabama 35809	10. PROGRAM ELEMENT, PROJECT, TASK AREA & WORK UNIT NUMBERS: DA 1L362303A214, AMCMS 632303.2140311.04
11. CONTROLLING OFFICE NAME AND ADDRESS: Commander, US Army Missile Command, Attn: DRDMI-TI, Redstone Arsenal, Alabama 35809	12. REPORT DATE: 15 July 1977
	13. NUMBER OF PAGES: 50
14. MONITORING AGENCY NAME & ADDRESS (If different from Controlling Office): 50pp.	15. SECURITY CLASS. (of this report): Unclassified
	15a. DECLASSIFICATION/DOWNGRADING SCHEDULE

16. DISTRIBUTION STATEMENT (of this Report)

Cleared for public release; distribution unlimited.

17. DISTRIBUTION STATEMENT (of the abstract entered in Block 20, if different from Report)

18. SUPPLEMENTARY NOTES

19. KEY WORDS (Continue on reverse side if necessary and identify by block number)

Submillimeter wave
Millimeter wave
Schottky-barrier diode
Superheterodyne receiver

20. ABSTRACT (Continue on reverse side if necessary and identify by block number)

This report reviews the current state-of-the-art performance figures for millimeter and submillimeter wave detectors and receiver systems. The frequency range under consideration is roughly 100 to 600 GHz. In contrast to the microwave (and optical) region where detectors perform close to the ideal limit, present millimeter and submillimeter wave detector sensitivities are one to two orders of

ABSTRACT (Continued)

over

DD FORM 1 JAN 73 1473 EDITION OF 1 NOV 65 IS OBSOLETE

UNCLASSIFIED

SECURITY CLASSIFICATION OF THIS PAGE (When Data Entered)

ABSTRACT (Concluded)

magnitude away from the ideal. This situation does not represent any fundamental limitation but rather reflects technological problems in detector and source development peculiar to this region of the spectrum. At the present time, rapid technological progress is occurring as a consequence of (1) the demand from fields such as radio astronomy, fusion diagnostics, and high resolution radar, and (2) the breakthroughs in microelectronic techniques, ultra-high frequency solid-state sources, tubes, and lasers. These developments are reviewed and the implications for millimeter wave radar systems are discussed.

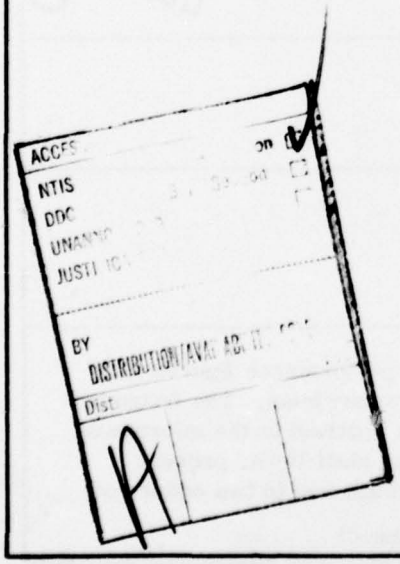

CONTENTS

PREFACE

This study was performed for the Advanced Sensors Directorate, US Army Missile Research and Development Command and was supported by the Scientific Services Program, Task Order No. 77-69 for the Battelle-Columbus Laboratories (Durham Operations) under US Army Research Contract No. DAAG29-76-D-0100. Dr. Waldman is an Associate Professor of Physics at the University of Lowell, Lowell, Massachusetts.

I. INTRODUCTION

MIRADCOM is engaged in the development of missile guidance links operating in the millimeter wave spectral region. Since system performance is directly related to component performance, it is necessary that present device performance be established and future device performance be predicted. To accomplish this, MIRADCOM is engaged in an assessment of millimeter and submillimeter device technology. This report reviews the status of sensors capable of operating in the region between approximately 100 and 600 GHz. State-of-the-art sensitivities are reported and an assessment of future performance is made. Background material is provided wherever possible to put performance figures in their proper context. Detectors which have inherently slow response times are not included in the report as no role can be foreseen for these detectors in radar and missile guidance systems. However, fast photoconductive detectors are considered in some detail because of their future potential, rather than their present performance.

A separate report on pyroelectric detectors is in preparation and will be available shortly.

II. SUMMARY

The present status of millimeter and submillimeter wave (100 to 600 GHz) sensors is reviewed in this report. Fundamental limitations to receiver sensitivity and their origins are discussed and compared for the two basic methods of detection: direct (or video) and superheterodyne (mixing the signal with a local oscillator and detecting at the difference frequency). Performance figures for detectors operating in both modes are presented.

For those detectors where data are available, namely room temperature Schottky-barrier diodes and liquid helium coded InSb photoconductors, superheterodyne noise-equivalent-power (NEP) is seven to eight orders of magnitude greater than video NEP. For this reason the main focus of attention by scientists and engineers requiring high sensitivity in detecting millimeter radiation has been on superheterodyne receivers and, in particular, on receivers using Schottky-barrier diodes as the mixer element. This interest developed as a consequence of the success of solid-state engineers in fabricating small-contact-area, low-capacitance Schottky diodes capable of rectifying at these very high frequencies. As a result, primarily of radio astronomers and their colleagues who design receivers, the performance level of room temperature GaAs Schottky-barrier diode superheterodyne receiver systems has improved dramatically during the past two to three years. At the present time, the best

room temperature receiver NEP at a frequency of 300 GHz is only one order of magnitude above the fundamental limit resulting from noise due to thermal background radiation. Of course, results are even better at lower frequencies. Based on the rapid rate of progress, one can anticipate further near-term improvements. Therefore, for frequencies up to 300 GHz, there does not appear to be any urgent need to develop new detector systems; GaAs Schottky-barrier diodes and perhaps silicon Schottky's as well should perform near the ideal limit.

However, the best receiver systems are generally one-of-a-kind, operating at radio astronomy facilities, and components (such as the high frequency diodes) are not readily obtainable. Therefore, support is strongly recommended to speed up the conversion of scientific realizability into commercial availability in this area, including support for the development of stable high frequency sources, which are required as local oscillators in superheterodyne receiver systems. At the present time, the sensitivity of systems using Schottky-barrier diodes and operating above approximately 150 GHz is limited by the lack of sufficient local oscillator power, and source development here would immediately improve receiver performance. In addition, the millimeter wave planar Schottky-barrier detector (a very recent development which is discussed in Section IV.D) deserves attention because of its considerable potential in missile receiver systems.

Alternatives to Schottky's for use in superheterodyne systems are reviewed in this report. They are Josephson junctions and bulk photoconductors, both of which require liquid helium temperature for operation. The InSb receiver system (discussed in Section VI.F) indicates the capabilities of bulk photoconductors for broadband performance (InSb will operate anywhere between 100 to 1000 GHz) and near-ideal sensitivity. However, a photoconductive material where the carriers have a shorter relaxation time (approximately 5 nsec instead of the 0.4 μsec relaxation time in InSb) is probably required for radar system applications, and support of solid-state research in this area is recommended.

Direct detection capabilities of a number of detectors is reviewed, including Schottky-barrier diodes, Josephson junctions and InSb, GaAs and silicon negative donor ion photoconductors. A reasonably sensitive, fast room temperature video detector would be highly desirable for terminal homing applications (e.g., as a sensor on the missile). While the Schottky detector holds considerable promise for satisfying this need, its millimeter wave video performance capabilities have been largely overlooked, and a research effort in this area is necessary.

Josephson junction detectors have existed for more than a decade. While the extraordinary versatility of the devices for generating, detecting, and amplifying millimeter and submillimeter waves have been demonstrated, the devices have not found any system applications. Millimeter wave astronomy can be viewed as a testing ground for future millimeter radar sensors because the receiver requirements of high sensitivity, field reliability, and large bandwidth exist in both areas. There are isolated cases of the application of Josephson junctions in millimeter wave astronomy, and these should be followed carefully and perhaps even supported to some extent. However, until the devices demonstrate superior capabilities in this field, their application in radar systems remains suspect.

III. VIDEO AND SUPERHETERODYNE RECEIVER PRINCIPLES

A. Comparison of Sensitivity Capabilities of Superheterodyne Receivers and Video Detectors in the Millimeter and Submillimeter

Video or direct detection of radiation implies a linear relationship between output voltage, V_S, and signal power, P_o; that is

$$V_S = RP_S \tag{1}$$

where R is the detector responsivitity in volts/watt. By mixing the signal P_S with a strong local oscillator source, P_{LO}, in a nonlinear element, a voltage at the difference frequency, $|\nu_S - \nu_{LO}|$, will be generated equal to

$$V_S = R\,(2P_S P_{LO})^{1/2} \quad . \tag{2}$$

The process of mixing and detection at an intermediate frequency (IF) is known as superheterodyne detection.

A comparison of Equations (1) and (2) indicates the advantage that can be achieved by mixing and converting local oscillator power to signal voltage. A quantitative comparison depends on analysis of the significant sources of noise in the frequency region of interest. Table 1 [1] lists the noise components that have to be considered in millimeter and submillimeter wave detection. The

TABLE 1. NOISE SOURCES FOR MILLIMETER AND SUBMILLIMETER DETECTORS [1]

No.	Noise Source	Theoretical Value (rms V)	Remarks
1	Amplifier	$\Delta V_A = 2(kT_A r_N B)^{1/2} = 7.43 \times 10^{-12}(T_A r_N B)^{1/2}$	
2	Johnson noise in detector	$\Delta V_J = 7.43 \times 10^{-12}(T_D r_D B)^{1/2}$	
3	Shot noise in detector bias current	$\Delta V_I = (2eIB)^{1/2} r_D = 5.7 \times 10^{-10}(IB)^{1/2} r_D$	
4	Fluctuation in local oscillator power	$\Delta V_L = R \cdot \Delta P_L = R\{2(h\nu/\eta)BP_L\}^{1/2}$	Assumes that optimum value for $P_L \sim r_r I^2$ the dc biasing power
5	Fluctuation in signal power	As 4 with P_L replaced by P_S	Normally, $P_S \ll P_L$
6	Fluctuation in background radiation incident on the detector	$\Delta V_B = 2Rh\nu\left[\frac{2\pi A}{\lambda^2}\frac{\sin^2\alpha}{(e^x-1)^2}\frac{e^x}{}B\Delta\nu\right]^{1/2}$ $\rightarrow 2RkT\left[\frac{2\pi A}{\lambda^2}\sin^2\alpha\ B\Delta\nu\right]^{1/2}$ when $x = h\nu/kT \ll 1$	
7	Fluctuation in the components of background radiation beating with the local oscillator	$\Delta V_b = R\left(2P_L P_b\right)^{1/2}$ where $P_b = \frac{2h\nu B}{e^x - 1}$ $2kTB$ when $x \ll 1$	This assumes both sidebands contribute, i.e., effective bandwidth = 2B

Note — Symbols and numerical values for Table 1 are given as follows:

A = area of receiving aperture of detector cryostat (cm^2)

α = half-angle of cone defining field-of-view of detector collection optics (rad)

B = post detector bandwidth (Hz)

e = electronic charge (coulombs)

η = quantum efficiency of detector (dimensionless ratio)

h = Planck's constant (Jsec)

I = bias current in detector (amps)

k = Boltzmann's constant (J/K)

λ = wavelength (cm)

ν = frequency (Hz)

$\Delta\nu$ = RF bandwidth of receiver (Hz)

P_L = local oscillator power (W)

P_S = signal power (W)

P_b = background power within receiver sidebands (W)

R = responsivity of detector (V/W)

r_D = resistance of detector (Ω)

r_N = equivalent noise resistance of amplifier (Ω)

T_A = amplifier temperature (K)

T_D = detector temperature (K)

T = temperature of background seen by the detector (K)

$\left.\begin{matrix}\Delta V_A \Delta V_J \\ \Delta V_T \Delta V_I \\ \Delta V_L \Delta V_B \\ \Delta V_b\end{matrix}\right\}$ = rms noise voltages at output of detector (V)

$x = h\nu/kT$ (dimensionless quantity)

effect of a particular noise source may depend on whether the detector is employed in the video or superheterodyne configuration. For example, fluctuations in background radiation incident on the detector produce the following noise voltages:

$$V_N = R\,kT\,(2B_1\,\Delta\nu)^{1/2} \qquad \text{(video case)}$$

and

$$V_N = R\,(4kTB_2P_{LO})^{1/2} \qquad \text{(superheterodyne mode)}$$

where

$\Delta\nu$ = spectral bandwidth to which the detector responds

B_1 = post detection bandwidth (typically 1 Hz)

B_2 = bandwidth of the IF amplifier in the superheterodyne receiver

R = detector responsivity.

Consider a simple example which illustrates the differences between video and superheterodyne detection. Assume that the dominant noise source produces the same noise voltage, V_N, for both cases (e.g., amplifier noise). A reasonable value for amplifier noise voltage is $V_N = 1 \times 10^{-9}$ V for a 1 Hz bandwidth. Also, let the detector responsivity, R, be 10^2 V/W and the optimum local oscillator power, P_{LO}, be 10^{-3} W. The minimum power detectable by the video receiver is then obtained by equating V_S to V_N in Equation (1) giving

$$P_S = \frac{V_N}{R} = 10^{-11}\ \text{W}$$

for a 1 Hz bandwidth (video receiver).

The minimum detectable power in the superheterodyne case is given by

$$P_S = \frac{(V_N)^2}{R^2 P_{LO}} = 10^{-19}\ \text{W}$$

for a 1 Hz bandwidth (superheterodyne receiver). Thus, the superheterodyne receiver is eight orders of magnitude more sensitive than video detection for the example chosen[1], although it should be realized that simple comparisons such as this cannot adequately characterize the differences that exist between superheterodyne and video detection systems.

Because of their much greater sensitivity (and complexity), millimeter wave superheterodyne systems have received more attention and, as a result, reliable noise figures are readily available in the open literature for the entire millimeter region. For certain video detectors (specifically, Schottky diodes and point contacts), one finds considerable variation in reported sensitivities. This problem will be considered in detail in Section IV.C.

While superheterodyne detection does provide a significant advantage for the detection of weak, narrowband signals which occur in active radar receiver systems, video detection ultimately becomes the more sensitive method for passive, broadband radiometry measurements. In this mode of operation the signal received, P_S, is proportional to the bandwidth, B, since the source acts as a broadband radiator at some effective temperature, T_S, which may be greater or less than the temperature of the surrounding environment, T_0. The signal voltage, V_S, is then directly proportional to the bandwidth for video radiometry reception but proportional only to the square root of the bandwidth for superheterodyne detection, as a comparison of Equations (1) and (2) indicates. When the correct dependence of noise voltage on bandwidth is accounted for, it can be shown that the minimum detectable temperature differential, ΔT_{min}, is proportional to $1/B$ for video radiometry and $1/B^{1/2}$ for superheterodyne radiometry [2]. Thus, for a sufficiently wide bandwidth, video detection becomes more sensitive. Figure 1 shows a comparison of video and superheterodyne millimeter wave radiometers in terms of ΔT_{min}.

---

[1] The values of R and P_{LO} are roughly those appropriate to Schottky-barrier diodes in the millimeter.

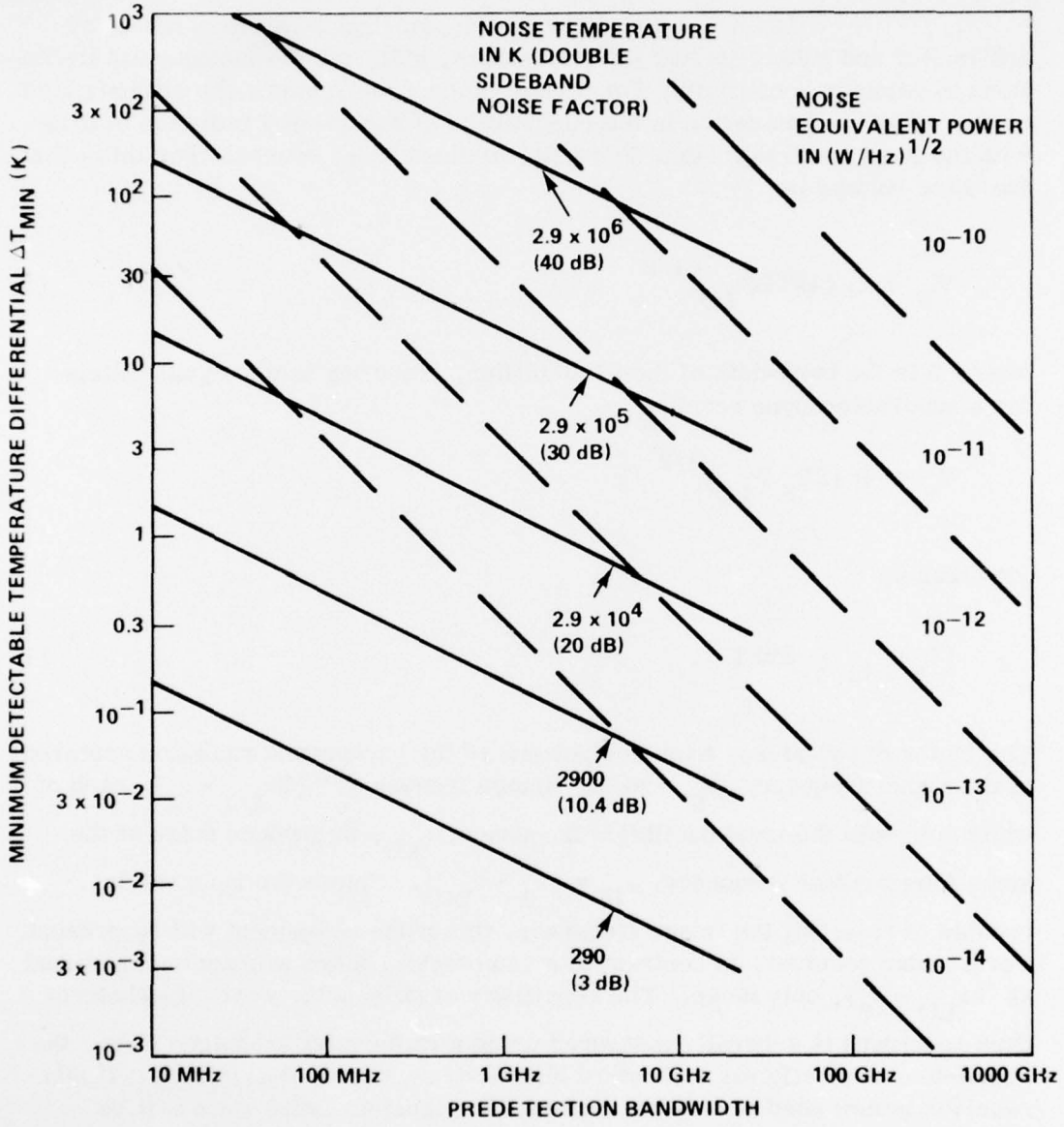

Figure 1. Comparison of long-wavelength heterodyne and direct-detection radiometers ($h\nu \leq kT$; post-detection integration time = 1 sec) [2].

B. Sensitivity Limit of Superheterodyne Systems and Receiver Noise Figure

Table 1, which lists all the principal sources of noise for millimeter and submillimeter wave detectors, indicates the fundamental limitations to detector sensitivity. For a superheterodyne system, the ultimate limit occurs when the fluctuation in the components of background radiation beating with the local oscillator (item 7) is the dominant noise source. For this case the noise voltage is

$$V_B = R\,(4kTBP_{LO})^{1/2} \tag{3}$$

where B is the bandwidth of the IF amplifier. Equating to the signal voltage for a superheterodyne receiver,

$$V_S = R\,(2P_S\,P_{LO})^{1/2} \quad ,$$

one obtains,

$$(P_S)_{min} = 2BkT \quad . \tag{4}$$

The factor of two arises from components of the background radiation centered at the signal frequency, ν_S, and the "image frequency," $(2\nu_{LO} - \nu_S)$, each of which mix with the local oscillator frequency, ν_{LO}, to produce noise at the same intermediate frequency, $\nu_{IF} = |\nu_S - \nu_{LO}|$. Unless the receiver is capable of rejecting the image frequency, this noise component will be present. For a radar receiver, in contrast to a radiometer, there will not be any signal at $(2\nu_{LO} - \nu_S)$, only noise. The sensitivity of millimeter wave superheterodyne receivers is generally measured using a radiometer technique (i.e., the signal-to-noise ratio for a standard blackbody source is determined). If this receiver is now used in a radar system, the signal-to-noise ratio will be degraded by a factor of 2 (3 dB). For these reasons it is necessary to specify both the sensitivity of the receiver and the mode of operation, i.e., double sideband (radiometer) or single sideband (radar), when quoting a system performance figure.

Equation (4) gives the sensitivity limit of an ideal (i.e., one which generates no internal noise) superheterodyne receiver. At the reference temperature of 290 K, $(P_S)_{min} = 4 \times 10^{-21}$ W/Hz. The effective bandwidth, here, is b = 2B. The additional noise contributed by the receiver is defined as the receiver noise temperature, T_N. The receiver noise figure, F, is then defined by

$$F_N = \frac{T_N + 290}{290} = \frac{T_N}{290} + 1 \quad . \tag{5}$$

Thus, the receiver noise figure, F, represents the ratio of an actual receiver's NEP to the ideal NEP. It is usually expressed in decibel; i.e.,

$$F_N\,(\mathrm{dB}) = 10 \log\left(\frac{T_N}{290} + 1\right) \quad .$$

Several types of detectors have been successfully employed as mixers in millimeter wave superheterodyne receivers. The most promising are room temperature GaAs and silicon Schottky diodes, GaAs, silicon and germanium point contact detectors, Josephson junctions, and InSb photoconductors. The performance characteristics of these detectors will be reviewed.

IV. SCHOTTKY-BARRIER DIODES

A. Introduction

The Schottky-barrier diode is the most widely used mixer element in state-of-the-art millimeter superheterodyne receivers. Its use, which has progressed to the millimeter region over the past decade [3,4], has been extended to submillimeter wavelengths by Fetterman et al. [5,6], who measured the heterodyne and video detection and harmonic mixing capabilities of low-capacitance small-contact-area GaAs Schottky diodes between 300 and 3000 GHz. The results indicated a heterodyne and video sensitivity superior to the point contact detector, and opened up the possibility of a number of submillimeter measurements in radio astronomy, plasma diagnostics [7], and imaging radars [8], which require receivers having both high speed (large bandwidth) and high sensitivity. Extension of Schottky diode detection to even higher frequencies has been reported very recently by McColl and

Hodges [9,10]. Using electron lithographic techniques they fabricated 0.5 μ diameter GaAs Schottky diodes and detected radiation at frequencies up to 7200 GHz (42 μ). However, sensitivity at the highest frequencies is rather poor; the video NEP is approximately 1×10^{-5} W/(Hz)$^{1/2}$ at 42 μ, indicating that further technological advances are required to produce efficient Schottky diode detectors in this region.

The point contact detector, which can be viewed as a first generation Schottky-barrier diode, is no longer competitive. In the point contact the metal whisker is forced to play two roles; its tip forms the junction and the whisker completes the circuit. The Schottky diode separates these incompatible tasks, and the result is a more rugged, reliable, and reproducible detector. With the advance of microelectronic technology, the diode junction area has been reduced to the point where junction capacitances, C_j, are typically tens of femtofarads (1 femtofarard = 10^{-15} farads). With diode series resistance, R_S, in the range of 10 Ω, the detector cut-off frequency, ω_C, defined by

$$\omega_C = \frac{1}{R_S C_j}$$

is approaching 10,000 GHz [11]. Consequently, over the entire millimeter region at least, and perhaps into the submillimeter as well, one can anticipate virtually no fall-off in GaAs Schottky diode performance resulting from the detector's inherent speed of response. Problems do exist, however, in coupling radiation into the diode because of its small size and the difficulties in extending conventional waveguide techniques to wavelengths near and beyond 1 mm.

The structure of a Schottky-barrier diode designed for millimeter wave detection is shown in Figure 2. GaAs is the most commonly used semiconductor material because its higher mobility leads to a high cut-off frequency. Silicon is also used, and it is claimed that the ability to prepare silicon substrates with much higher doping densities (10^{20} cm^{-3} versus 10^{18} cm^{-3} for GaAs) compensates for its lower mobility [12]. However, experimental results to date favor GaAs Schottky's.

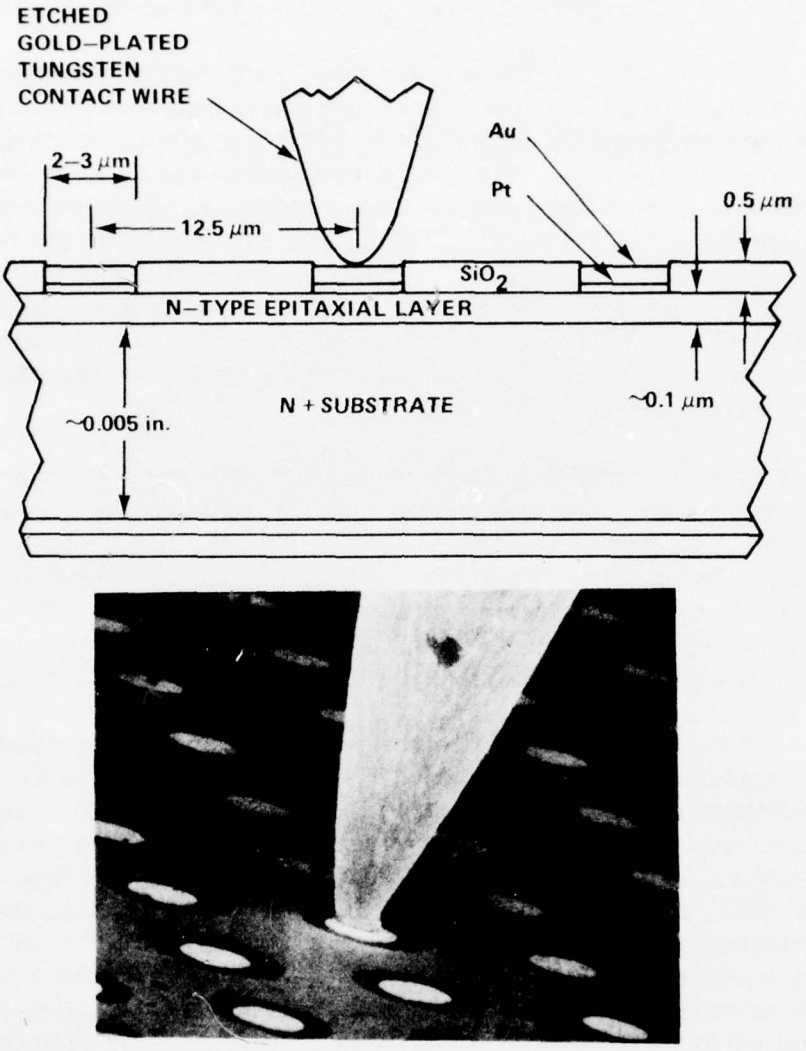

Figure 2. Top: Structure of the millimeter wave-contacted Schottky-barrier diode. The metal-semiconductor contact area is delineated photo-lithographically or electron-lithographically. Bottom: Micrograph of a typical diode array, one diode of which is being contacted by means of an etched wire under compression. Cold bonding between the wire and the diode metallization can be made to occur during packaging, making the device quite rugged (adapted from Reference 12).

B. Schottky-Barrier Diode Superheterodyne Receiver Systems

During the past few years considerable progress has been made in improving millimeter wave superheterodyne receiver noise figures and a good beginning has been made in developing similar systems for submillimeter wavelengths. Most of these receivers use Schottky-barrier diode detectors as mixers, particularly GaAs Schottky's. Excellent performance has recently been achieved at 140 GHz [13], 170 GHz [14], 230 GHz [15,16], and very recently at 325 GHz.[2] It is interesting to note that millimeter wave superheterodyne receivers were operating in the atmospheric windows at 140 GHz and 230 GHz as far back as 1963 [17] with respectable noise figures [20 and 26 dB, respectively], and by 1966 a system was operating at 600 GHz with a noise figure of 33 dB [18].

In general, millimeter wave superheterodyne receivers have utilized fundamental mode waveguide and conventional waveguide techniques, although the trend at frequencies above 140 GHz is to employ quasi-optical components [19,20]. For example, Erickson employs an optical diplexer for efficiently coupling the signal and local oscillator into the mixer at 325 GHz. Other techniques which are being pursued include (1) diodes with antennas and diode arrays (see Section IV.D) and (2) millimeter wave integrated circuits [17].

The most promising alternatives to room temperature Schottky diodes for use as mixer elements are Josephson junctions [23] (Section V.C) and InSb photoconductors [24,25] (Section VI.F), both of which require liquid helium temperature for operation. Other potential superheterodyne detectors are: InSb Schottky diodes [26], superconductor-semiconductor (super-Schottky) diodes [27], pyroelectric detectors [28, 29, 30], novel photoconductive systems such as the silicon negative donor ion detector [31], and metal-oxide-metal detectors [32, 33]. None of these detectors have been utilized in millimeter or submillimeter superheterodyne receiver systems and, thus, there are no real performance data for them. The physics relevant to the operation of these detectors and, where data are available, their direct detection capabilities in the millimeter and submillimeter are reviewed in later sections of this report.

Table 2 summarizes the present status of millimeter and submillimeter wave superheterodyne receivers. Noise figures are quoted for complete packaged systems advertised for sale in trade journals (Hughes receivers at 94 and 140 GHz), as well as first generation laboratory receivers using optically pumped submillimeter wave lasers as local oscillators (Fetterman's results at 600 GHz). Table 2, although by no means complete, indicates the

---

[2] Neal R. Erickson, Department of Physics, University of California at Berkeley, private communication.

TABLE 2. NOISE FIGURES FOR MILLIMETER AND SUBMILLIMETER WAVE SUPERHETERODYNE RECEIVERS

Frequency (GHz)	Noise Figure (Noise Temperature)	System NEP (W/Hz)	Reference, Journal (if Appropriate), Year	IF Center Frequency	Operational Temperature (K)	Detector
94	6.5 dB	1.8×10^{-20}	Hughes Aircraft, Microwaves, April, 1977	Variable to 1 GHz	290	Silicon Schottky
115	740 K } Single sideband mixer noise		Kerr, MTT, Oct. 1975 [34]	1.4 GHz	290	GaAs Schottky
115	300 K } temperature only		Kerr, MTT, Oct. 1975 [34]	4.75 GHz	77	GaAs Schottky
120	2.7 dB (250 K)	7.4×10^{-21}	Phillips and Jefferts, RSI, Aug. 1973 [24]	2 KHz-2 MHz	4.2	InSb photoconductor
140	8.5 dB (1760 K)	2.8×10^{-20}	Hughes Aircraft, Microwaves, April 1977	Variable to 1 GHz	290	Silicon Schottky
140	3.8 dB (400 K)	9.6×10^{-21}	Wrixon, MTT, Dec. 1974 [13]	1.4 GHz	290	GaAs Schottky
170	1500 K Single sideband mixer noise temperature only		Kerr, MTT, May 1977 [14]		290	GaAs Schottky
175	8.1 dB (1570 K)	2.6×10^{-20}	Wrixon, MTT, Dec. 1974 [13]	1.4 GHz	290	GaAs Schottky
183	11 dB (3400 K)	5.0×10^{-20}	Gallagher, GA Tech, Private Comm. 1977	2 GHz	290	GaAs Schottky
185-300	Work in progress		Gustincic, SMM Conf. II, Proc., 1976 [19]		290	GaAs Schottky
220	16 dB	2.0×10^{-19}	Cotton, Alpha Ind., Private Comm., 1977	1.4 GHz	290	GaAs Schottky
230	13.4 dB (6000 K)	8.8×10^{-20}	Goldsmith, MTT, Nov. 1976, [16]	1.4 GHz	290	GaAs Schottky
230	13.4 dB (6000 K)	8.8×10^{-20}	Schneider and Wrixon, MTT Symp. 1974 [15]	1.5 GHz	290	GaAs Schottky
230	3.1 dB (300 K)	8.2×10^{-21}	Phillips and Jefferts, MTT, Dec. 1974, [25]	20 KHz-2 MHz	4.2	InSb photoconductor
300	8.0 dB (1320 K)	2.5×10^{-20}	Edrich, SMM Conf. II. Proc., 1976 [23]	9.0 GHz	4.2	Josephson junction
325	10.6 dB (3050 K)	4.6×10^{-20}	Erickson, Univ. of CA, Berkeley, Private Comm.	1.4 GHz	290	GaAs Schottky
600	27 dB (2×10^{5} K)	2.0×10^{-18}	Fetterman, Lincoln Labs, Private Comm., 1977	1.4 GHz	290	GaAs Schottky
2500	48 dB (2×10^{7} K)	2.5×10^{-16}	Norton, SMM Conf. II, Proc., 1976 [31]		2.0	Silicon photoconductor (negative donor ions)

Note — Noise figure is double sideband and refers to total system noise unless otherwise stated. System NEP for radar applications would be twice the value given in the table.

intense scientific activity in this field. The rapid progress being made is exemplified by the results of Schneider and Wrixon [15]. Their noise figure at 230 GHz is 7 dB below that of the 140 GHz receiver recently designed for the Army Ballistic Research Laboratories' beamrider experiments. Furthermore, it is now generally believed that for Schottky diode systems operating above about 150 GHz, noise figures are degraded by limitations in available local oscillator power [13, 15]. The local oscillator power necessary to optimize the receiver sensitivity is a function of coupling efficiency, which falls off rapidly at the higher frequencies. The actual LO power required at the diode appears to be in excess of several milliwatts. Wrixon [13] found that the LO power was insufficient because there was a 13 dB loss through the coupling cavity using a 35 mW klystron at 175 GHz. Schneider and Wrixon [15] use a doubled 150 mW, 115 GHz klystron as the LO for their 230 GHz receiver. They estimate that their doubler has an efficiency of 3 to 4%, and measure a rectified current of 2.5 mA with the mixer detector directly at the output of the multiplier.[3] On the basis of previous measurements with mixers at 140 GHz, they believe 2.5 mA of rectified LO signal is sufficient to minimize receiver noise figure. Thus, it would appear that approximately 5 mW of LO power at the detector is required to optimize millimeter wave Schottky-barrier diode mixers. Improvements in receiver design, increased efforts in developing compact and stable LO sources in the 150 to 300 GHz region, and/or more efficient millimeter wave doublers and triplers [35] should enable this power level to be reached in the near future. At present, however, this power requirement is one disadvantage of Schottky diodes relative to the helium-cooled Josephson junctions or InSb photoconductors for superheterodyne receivers operating above approximately 150 GHz. The cooled detectors are optimized, as mixers, at LO power levels of 10^{-7} to 10^{-6} W (see Sections V.C and VI.F).

A new technique known as subharmonic mixing [36-39] appears promising, based on results obtained in the 30 to 60 GHz region. Subharmonic mixing, which uses a pair of diodes in an antiparallel configuration, is a sophisticated modification of the more conventional harmonic mixing technique. The advantages claimed [36] for this configuration are:

1) Reduced conversion loss by supressing the fundamental mixing products.

2) Lower noise figure through supression of local oscillator noise sidebands.

---

[3] After inserting their coupling cavity, which had a 7 dB transmission loss, the rectified current fell to 0.3 mA, and they estimate that the then inadequate LO power adds 3 dB to the 230 GHz receiver noise figure.

3) Supression of video detection.

4) Inherent self-protection against large peak inverse voltage burnout.

Millimeter wave receivers using the subharmonic mixing technique are currently under development at a number of laboratories, including Hughes Aircraft.

Some effort has been directed at improving the performance of Schottky diode mixers by cooling. Under most conditions, the principal source of noise from a dc-biased Schottky-barrier is shot noise. In that case, the shot noise power is

$$P_{SN} = \frac{1}{2} q\, I R_x B$$

where

q = electronic charge

I = diode current

R_x = variable diode resistance

B = bandwidth.

For a diode at room temperature, the I-V characteristic can be written as $I = I_S e^{V/V_0}$. Assuming that thermionic emission is the dominant conduction mechanism, the constant V_0 is approximately

$$V_0 = \frac{kT}{q} \quad .$$

Therefore,

$$R_x = \left(\frac{dI}{dV}\right)^{-1} = \frac{V_0}{I} = \frac{kT}{qI}$$

and consequently,

$$P_{SN} = \frac{1}{2} kTB = kT_{eq}B \quad ,$$

where T_{eq} is the equivalent noise temperature of the diode. Thus, the noise power should decrease linearly with temperature. This will occur until the temperature is reduced to the level where field-emission dominates, at which point V_0 and P_{SN} become temperature independent. Actually, field emission contributes somewhat to conduction even at room temperature. Experimentally, what has been observed is a reduction in noise power of a factor of 2.5 upon cooling the mixer from 290 K to 77 K and no further reduction in cooling to 18 K [34], which is in reasonable agreement with the preceding arguments. The magnitude of the gain obtained by cooling appears to be inadequate to warrant its application to field radar systems.

In conclusion, one can expect continued progress in the near future for room temperature, millimeter wave Schottky diode superheterodyne systems operating up to and beyond 300 GHz as diode fabrication techniques, local oscillators, and receiver designs are improved.

C. Schottky-Barrier Diode Video Detectors

A comparison of Equations (1) and (2) indicate that good mixers are good video detectors because the same detector responsitivity, R, determines mixer and video detector performance. For applications where fast response is not required, thermal detectors are useful and are widely employed as video receivers, whereas these same detectors would rarely be found in superheterodyne receivers because of their restricted bandwidth. The ideal millimeter wave detector would have a fast response, high sensitivity, and operate at room temperature and would, thus, be equally suitable for video or superheterodyne reception. At the present time, such a detector does not exist, and one is forced to trade off high responsivity for fast response. However, progress in fabrication of millimeter wave Schottky diode detectors over the past decade has made this detector the most promising of the alternatives.

Figure 3 compares the state-of-the-art in diode performance in 1967 [40] with that at the present time. The present day results are based on an estimate from conversations with individuals intimately connected with millimeter wave Schottky diode development rather than published data and, as such, are probably uncertain by approximately a factor of 5. Nonetheless, the trend is unmistakable, i.e., an order of magnitude increase in the high frequency cut-off.

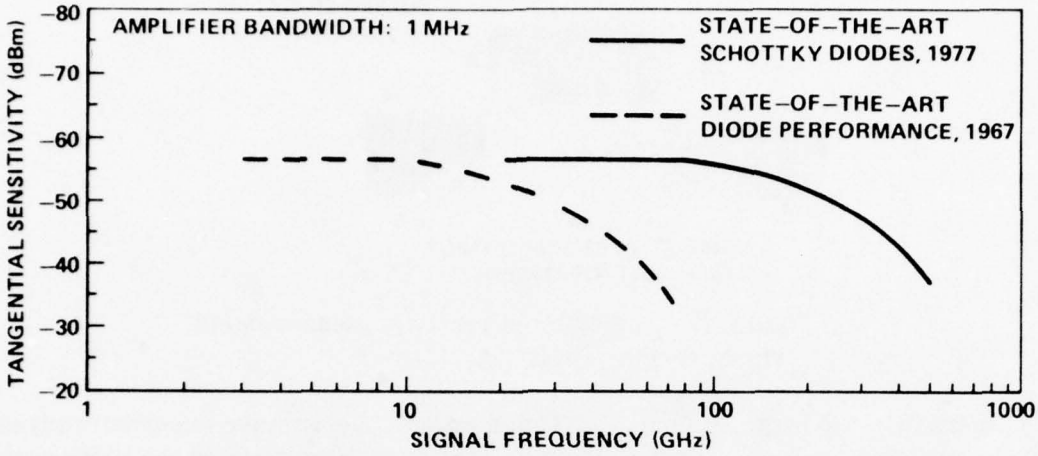

Figure 3. Tangential sensitivity versus signal frequency for good-quality detector diodes in 1967 [40] and 1977 (estimated).

The most common method of characterizing a video detector's sensitivity is to give its tangential sensitivity. The tangential sensitivity of a detector is essentially defined as the signal power required to generate a "reasonable" signal-to-noise ratio on a video display. The definition of reasonable is made semi-quantitative by specifying that the tangential sensitivity is that power level at which the highest noise peaks in the absence of a signal are at the same level as the noise peaks in the presence of the signal (Figure 4). A tangential sensitivity rating corresponds to a signal-to-noise ratio of approximately 2.5. Further, tangential sensitivity is usually defined for a particular bandwidth appropriate to the video amplifier employed. To convert to NEP in $W/(Hz)^{1/2}$, the common definition of detector sensitivity in the optical and infrared, we have

$$\frac{\text{tangential sensitivity}}{2.5\,(B)^{1/2}} = \text{NEP}$$

since video detector noise power increases as the square root of the bandwidth. Referring to Figure 3, the present GaAs Schottky diode provides a tangential sensitivity of approximately -55 dBm in a 1 MHz bandwidth at 140 GHz. The NEP is, therefore

$$\text{NEP} = 1.6 \times 10^{-12}\ W/(Hz)^{1/2} \quad .$$

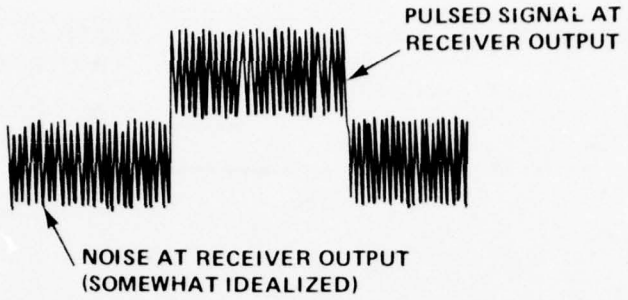

Figure 4. Tangential-sensitivity measurement visual display [40].

In contrast to the large number of articles on millimeter wave superheterodyne receivers using Schottky diodes, there is almost no literature on the video performance of these detectors. A recent article in Microwaves [41] quotes an NEP of 4.5×10^{-13} W/(Hz)$^{1/2}$, but no reference is given nor is the frequency specified. Generally, until a year ago, NEP's quoted in the literature were in the range of 10^{-9} to 10^{-10} W/(Hz)$^{1/2}$ [42]. However, there are isolated reports of higher sensitivities. In 1966, Bauer et al. [43] quoted an NEP of 5×10^{-12} W/(Hz)$^{1/2}$ at 280 GHz and 1.6×10^{-12} W/(Hz)$^{1/2}$ at 140 GHz for a silicon-tungsten point contact detector. Apparently, the very best point contact detectors are (for a short time at least) comparable in sensitivity to Schottky diodes. Part of the progress of the past 10 years has been to develop a reproducible and rugged version of the best point contacts.

In view of the simplicity of operation of video Schottky diodes, a number of applications in the millimeter region can be foreseen. Therefore, it would be very useful to have a complete, detailed study of the NEP of these detectors over the entire millimeter and submillimeter wavelength range.

D. Planar Schottky-Barrier Diode Detectors

Relative to point contact detectors, considerable improvement in performance, reliability, and ruggedness has been obtained by using microelectronic technology to fabricate Schottky diode detectors. However, while the etched whisker is no longer part of the junction, it still must be formed into a mechanically stable shape, which also serves as a high frequency antenna, and then be attached to the diode. In contrast to the diode fabrication, this process remains relatively unautomated and time consuming, and the ability of the thin whisker to survive unaffected in a high-g, high vibration environment is questionable.

One promising approach to overcoming these difficulties has been the fabrication of small, planar, surface-oriented Schottky diodes in which both terminals of the rectifying junction lie on the same surface of the semiconductor wafer. Devices with this topography, which can detect and mix at millimeter and submillimeter wavelengths, have recently been developed by Murphy et al. [44]. Mixing of the 82nd harmonic of an X-band kylstron with a submillimeter laser has been observed in these devices, and direct detection capability at frequencies up to 2500 GHz (118 μ) has been demonstrated.[4] At this early stage of development, the planar diodes are roughly an order of magnitude less sensitive than conventional Schottky's designed for the millimeter and submillimeter wavelength range, but one can anticipate improvements in sensitivity as the planar diode design is optimized. Furthermore, their simplified geometry may allow them to be designed into configurations totally different from conventional Schottky's. A scanning electron micrograph and a schematic of this device are shown in Figure 5.

The planar topography of these devices suggests a number of applications. Figure 6 shows an array of planar diodes on a single GaAs wafer. These diodes can be individually contacted and signals reaching them processed electronically in a number of ways. This could provide a method of efficient coupling to the

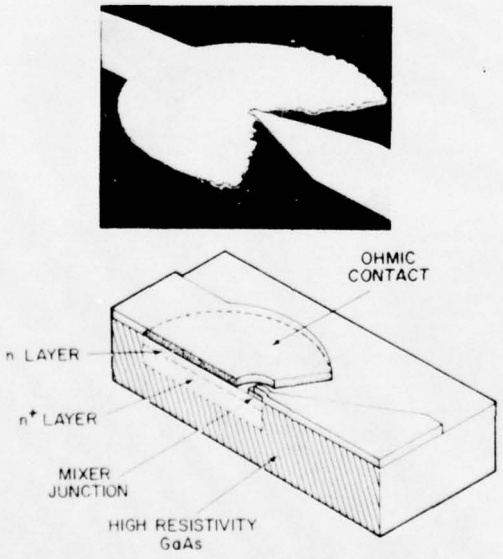

Figure 5. Top: Scanning electron micrograph showing 2 μm diode (small dot in center), ohmic contact establishing connection to n^+ layer of diode, and two metal strip contacts. Bottom: Planar diode as fabricated by growth of n-n^+ epitaxial layers on a high-resistivity GaAs substrate [44].

[4] H. R. Fetterman, MIT, Lincoln Laboratory, private communication.

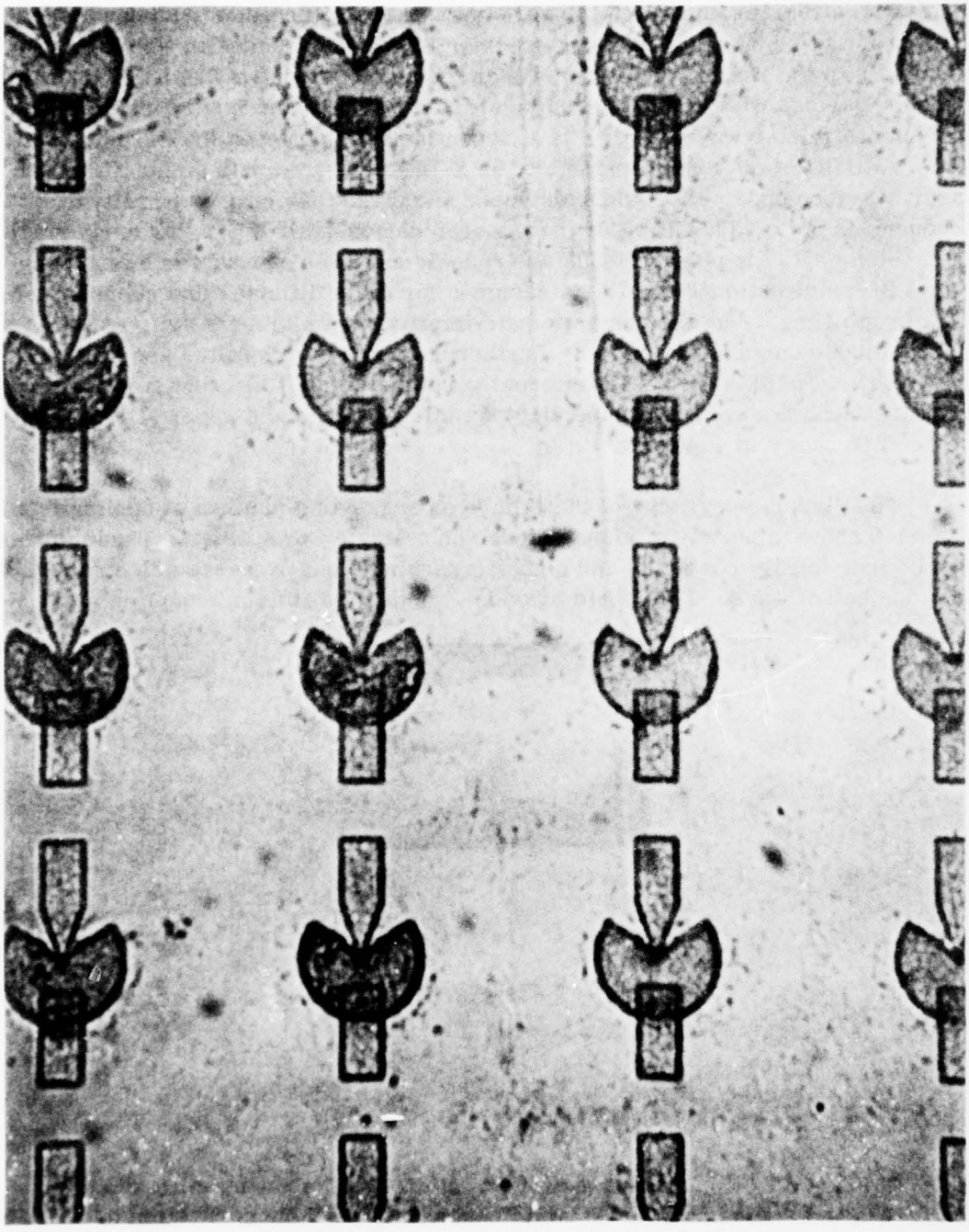

Figure 6. An array of planar diodes on a GaAs wafer. The diode is located at the tip of the arrow-shaped printed wire and has a diameter of approximately 2 μm.

free space radiation mode or, possibly, the detector array for a millimeter wave imaging system. Another potential application for these devices is indicated by Figure 7 which shows a micrograph of four planar diodes on a GaAs wafer. The whiskers on the elements are fabricated to dimensions corresponding to a half wavelength for four different submillimeter laser sources to provide an antenna structure for efficient radiation coupling into the junction. The leads at right angles to the antenna and the rectangular pads are designed (for mixer applications) to present a high impedance to the signal and a low impedance to the IF frequency. Polarization selectivity is another possible application suggested by Figure 7. These concepts are still in the early research stage and data are not yet available.

V. JOSEPHSON JUNCTION DETECTORS

A. Introduction

A number of unusual effects, which can be utilized for the detection of millimeter wave radiation, occur when current flows through a barrier between two superconductors. The phenomena, predicted by Josephson [45], result from the phase difference, $\delta\phi$, between the wave functions for paired electrons which describe the macroscopic superconducting quantum states on each side of the junction. Figure 8a is an example of the design of a simple Josephson point contact junction. The oxide barrier between the niobium tip and wire is typically 10 to 20 Å. Other types of Josephson junctions which are currently under study are the superconductor-insulator-superconductor (SIS) thin-film junction and the superconductor-normal metal-superconductor (SNS) junction, both of which can be fabricated with planar integrated technology. The geometry of these devices is shown in Figure 8b. While the latter devices hold promise for solving many of the problems associated with Josephson junction point contact detectors (namely, fragility, sensitivity to vibration and electrical noise, variation in operating characteristics from detector to detector, and degradation in performance after thermal recycling), up to the present time the point contact Josephson junction is the only type that has been used successfully as a detector of millimeter wave radiation. In contrast to the (SIS) and (SNS) junctions, the point contact has a relatively high impedance (ten to several hundred ohms), which couples well to the radiation field, and a junction capacitance small enough to allow the detector to respond to frequencies as high as 1000 GHz [47].

Figures 9 and 10 show the idealized I-V curves of a typical point contact Josephson junction without dc and with ac exposure to microwave radiation. The striking differences between the ac and dc curves suggest the unique potential of the Josephson junction for millimeter wave technology — as a

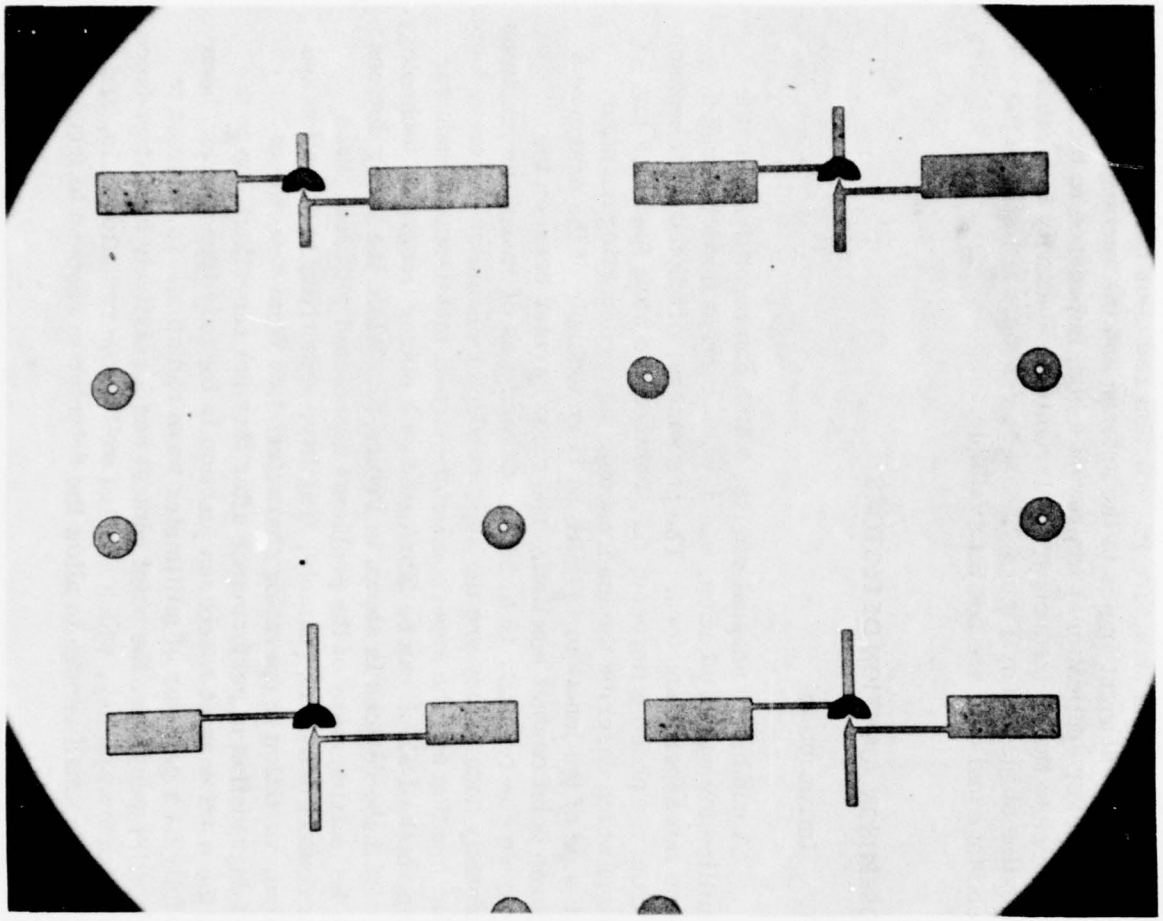

Figure 7. An array of four planar diodes. The vertical printed wires have been dimensioned to correspond to a half wavelength for four different submillimeter laser sources to provide an antenna structure for coupling radiation into the junction.

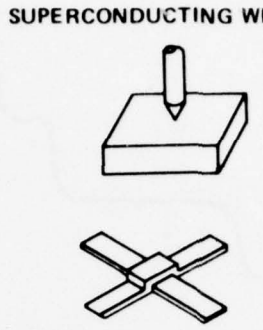

Figure 8. Top: Point contact between two superconductors. Bottom: Sandwich junction in which the barrier may be 10 to 30 Å of insulating oxide (SIS) or several thousand angstroms of a normal metal (SNS) [46].

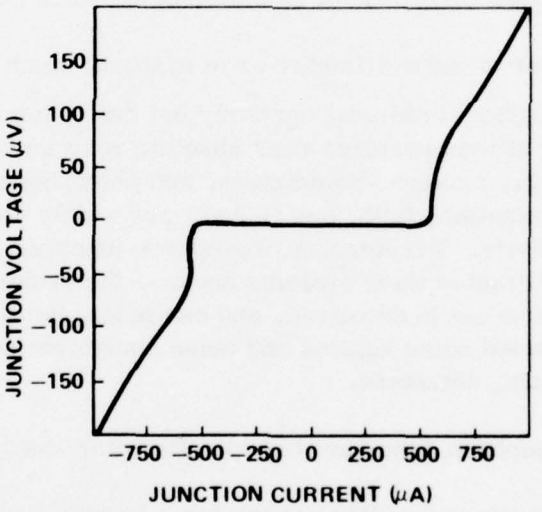

Figure 9. Current-voltage curve for an Nb-Nb point contact Josephson junction at 4.2 K [48].

sensitive, broadband, and high-speed video detector [48], as the mixer element in a heterodyne receiver [49], a voltage tunable narrowband detector [50], a parametric amplifier [51,52], and even a millimeter and submillimeter source [53]. Unfortunately, while all of these capabilities have been demonstrated in principle during the past decade, there are at the present time

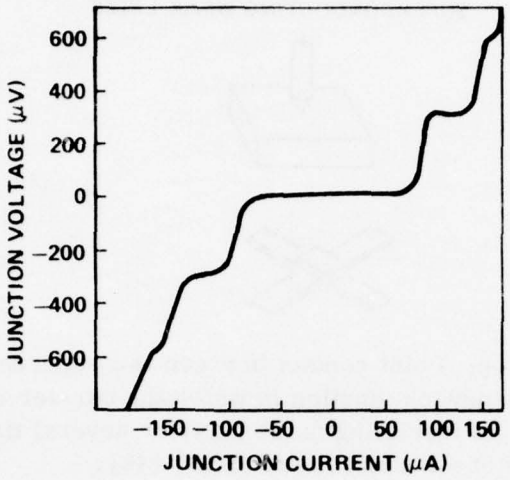

Figure 10. I-V curve for an In-In point contact Josephson junction in the presence of 10^{-9} W of radiation at 150 GHz [48].

virtually no millimeter or submillimeter wave systems which use Josephson junctions.[5] This situation is almost certainly not due to the difficulties associated with operating at temperatures near absolute zero since other low temperature devices [e.g., masers, bolometers, and photoconducting far infrared detectors (doped germanium, InSb, and GaAs)] are widely used in systems requiring high sensitivity. Presumably, Josephson junctions have not been incorporated into millimeter wave systems because the problems of reliability and reproducibility have not been solved, and one must take this into account when comparing reported noise figures and noise equivalent powers of Josephson junctions with competing detectors.

B. *Josephson Junctions — Video Detector Performance*

The current-voltage curve for a Josephson junction biased with a dc voltage is shown in Figure 9. The resistance of the junction is zero for currents less than I_0, the maximum zero voltage current. For $I < I_0$ only

---

[5] One notable exception is the recent development by Edrich [23] of a 315 GHz Josephson junction receiver, with a double sideband system noise temperature of 1320 K. This system is planned for installation on the 36-foot radio-telescope of the National Radio Astronomy Observatory in Tucson, Arizona, within the next 2 years.

supercurrents flow (i.e., electron pairs). For $I > I_0$ there is a transition to normal resistance, and both normal currents and supercurrents flow. The effect on the junction of an incident electromagnetic field is quite complex, as Figure 10 indicates. For broadband video detection applications, the important point is that the applied radiation reduces the maximum zero voltage current and, thus, by biasing the junction with a constant current source at a value just above I_0, a voltage proportional to the incident field intensity is generated (Figure 11).

Figure 12 shows the broadband millimeter wave response of a Nb-Nb Josephson junction point contact detector [47] at 4.2 K. This is not a detector response curve but a system response, which includes detector, blackbody source, and interferometer. However, the high frequency cut-off at approximately 500 GHz is a detector characteristic. Ignoring the large peaks in the responsivity between 100 and 200 GHz, the envelope of the curve is relatively flat to 500 GHz. As a rough approximation, one can assume that the source energy increases as the square of the frequency in this region and that the interferometer has a flat response. Thus, the detector responsivity is generally varying as $1/\nu^2$, probably as a result of the decreasing impedance presented to the radiation by the junction capacitance. Blaney [47] notes that, "the response curve does not represent all Nb-Nb junctions operating at 4.2 K." That is, the frequency dependence of the responsivity of Josephson junction point contacts is not understood at present. Despite these uncertainties, the best sensitivity figures for Josephson junction millimeter wave detectors are impressive. The results given in Table 3 indicate that the best Josephson junctions have an NEP at least as low as the best cooled bolometers for wavelengths of 1 mm and longer and, being fast, have a much greater bandwidth capability.

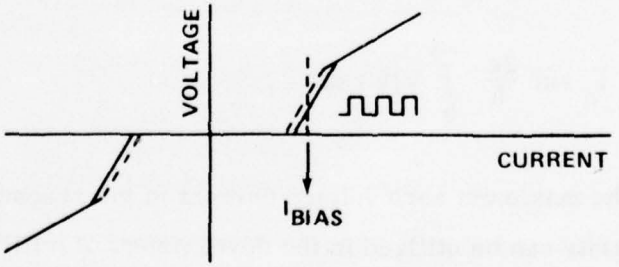

Figure 11. Schematic I-V curve showing how applied radiation changes the zero voltage current, so that a chopping beam results in a modulated voltage. In the absence of radiation the full curve is observed, but the application of radiation reduces the maximum zero voltage current and shifts the curve to the dashed position. A constant current external source sets the operation at a point of high slope [64].

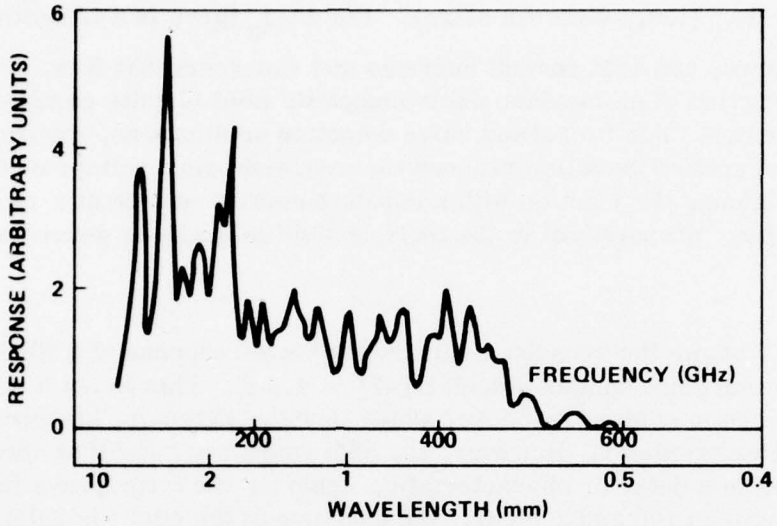

Figure 12. Variation with frequency of the response (in arbitrary linear units) of an Nb-Nb point contact to radiation from a mercury discharge lamp as measured by a lamellar grating interferometer. Nominal resolving power, 7.5 GHz; junction temperature, 4.2 K; constant current bias giving a nominal dc voltage of 50 μV (Josephson frequency 24 GHz); maximum signal level, $\approx 5\,\mu$V; and post-detection time-constant, 1 sec [47].

C. Josephson Junctions — Superheterodyne Receiver Performance

When a Josephson junction is biased with electromagnetic radiation, an exceedingly complex nonlinearity is developed between current and voltage, i.e.,

$$I(t) = I_c \sin \frac{2e}{\hbar} \int_0^t V(t')\, dt'$$

where I_c is the maximum zero voltage current in the absence of radiation. This nonlinearity can be utilized in the development of millimeter wave Josephson junction mixers. The Berkley group of Taur et al. [49], has reported noise figure measurements at 36 GHz using a point contact Josephson junction as a mixer. Kanter [54] at Aerospace has made similar measurements at 95 GHz and Edrich [23] recently reported results at 300 GHz. The latter results

TABLE 3. SOME VIDEO DETECTION PROPERTIES OF POINT CONTACT JOSEPHSON DETECTORS [47]

Property	Performance
Operating temperature	below $\sim$ 10 K
Frequency range	up to $\sim$ 1 THz (0.3 mm)
Radiation power level	$\lesssim 10^{-8}$ W (at λ = 3 mm)
Responsivity	up to 10^{5} V W^{-1} (at λ = 3 mm)
Noise equivalent power (best achieved)	5×10^{-15} $W(Hz)^{-1/2}$ (at λ = 3 mm)
	10^{-14} $W(Hz)^{-1/2}$ (at λ = 2 mm)
	5×10^{-14} $W(Hz)^{-1/2}$ (at λ = 1 mm)
Response time	$\gtrsim 10^{-8}$ sec (direct measurement)
	$\gtrsim 10^{-10}$ sec (inferred from mixing experiment)

are contained in Table 2, the summary of state-of-the-art noise figures for millimeter wave superheterodyne receivers.

Kanter's conclusion is that both the noise figure and frequency dependence of Josephson junctions are comparable to that of cooled[6] Schottky diodes, and, therefore, they do not offer any advantage over Schottky's when used as mixers. His opinion is that the real opportunity for Josephson junctions resides in their use as active parametric amplifiers. This statement overlooks the greatly reduced local oscillator power requirements of Josephson junctions as compared to Schottky's (10^{-6} W versus 10^{-2} W). Because local oscillator power is not readily available above 150 GHz at the present time, Josephson junction receivers should out-perform Schottky receivers at these frequencies. Edrich's double sideband noise temperature of 1320 K at 300 GHz, using a point contact

[6]Because Josephson junctions must, of necessity, operate near liquid helium temperature, their sensitivity should be compared with the corresponding results for cooled semiconductor diodes. Measurements on cooled Schottky diodes have been made by Weinreb and Kerr [55] and are contained in Table 2.

Josephson junction as the mixer, a maser as the IF amplifier, and a tripled klystron as the local oscillator, tends to confirm this. However, as LO power increases, Schottky diode receivers should attain at least the same performance level at this frequency.

VI. MILLIMETER AND SUBMILLIMETER WAVE PHOTOCONDUCTIVE DETECTORS

A. Introduction

At or near liquid helium temperature, many high purity semiconductors (including Ge, Si, GaAs, and InSb) become fast, rugged, and sensitive detectors of millimeter and submillimeter radiation. A number of different physical properties can come into play at low temperatures which enable electrons distributed throughout the bulk of the semiconductor material to absorb radiation in this regime and thereby change their state in such a way that their mobility in the sample is altered, leading to a photoconductive signal.

The most common process utilized is called extrinsic photoconductivity. In this technique electrons (holes) bound to donor (acceptor) impurity sites by a hydrogen atom-like potential are excited into the conduction (valence) band. The electrons (holes) thus freed are able to carry current and the conductivity of the sample increases. The ionization energy for hydrogenic impurity centers in semiconductors is approximately

$$E_{ioniz} = 13.6 \frac{m^*}{m_e \epsilon^2} \text{ (eV)}$$

where m^* is the effective mass of the free carrier in the semiconductor and ϵ is the dielectric constant. Small band gap semiconductors such as GaAs and, especially, InSb have small values of m^* and large dielectric constants, thus locating the ionization energy for donor impurity centers in the millimeter and submillimeter. For example, InSb has $m^* = 0.013\ m_e$, $\epsilon = 16$, and $E_{ioniz} = 0.7$ meV.[7] Unfortunately, binding energies this small imply very large hydrogenic orbits[8], and for InSb the Bohr radius is roughly 5.6×10^{-6} cm. As a

---

[7] 1 milli-electron volt (meV) $\approx 8.1\ \text{cm}^{-1} \approx 240$ GHz

[8] $a_{\text{Bohr Radius}} = 5.3 \times 10^{-9} \left(\frac{m^*}{m_e}\right) \epsilon$

result, if the impurity concentration is not less than approximately 10^{13} cm^{-3}, there exists sufficient interaction between adjacent orbiting electrons to delocalize them, and the distinction between bound localized electrons and free electrons in the conduction band vanishes. Because InSb has not as yet been produced at the required purity, extrinsic photoconductivity of this type has not been observed.

B. GaAs Extrinsic Video Photoconductor

For GaAs the purity requirements are reduced ($m^* = 0.065\ m_e$, $\epsilon = 12$), and extrinsic photoconductivity is observed [56,57] for donor impurity concentrations up to 1×10^{15} cm^{-3}. Optimum sensitivity occurs at a donor impurity concentration of 2×10^{14} cm^{-3} [57]. The frequency dependence of the responsivity curve is shown in Figure 13. The NEP at 35 cm^{-1} (the peak of the response curve) is 1×10^{-12} $W/(Hz)^{1/2}$. In common with all extrinsic photoconductors, the response exhibits a sharp low frequency cut-off, which for GaAs occurs at 25 cm^{-1} (750 GHz). This represents the low frequency limit

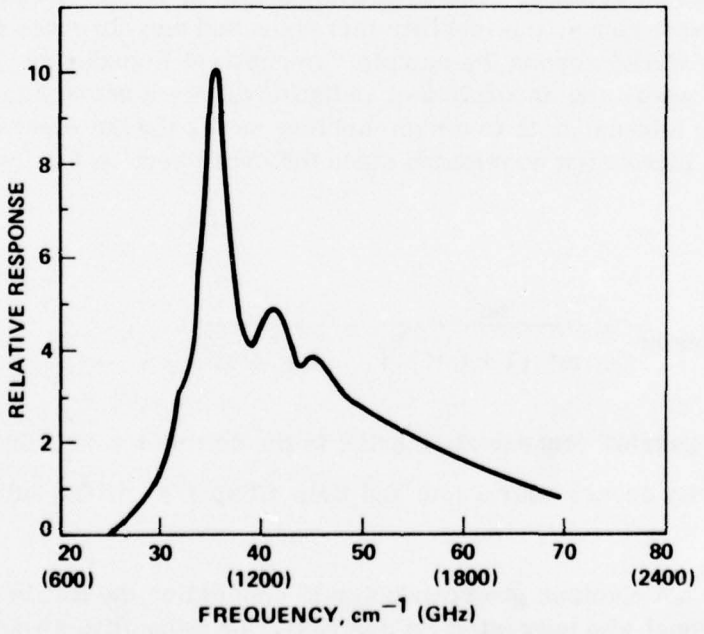

Figure 13. Extrinsic photoconductivity spectrum for high purity GaAs at 4.2 K. NEP at peak of response curve is approximately 1×10^{-12} $W/(Hz)^{1/2}$ [57].

of extrinsic photoconductive detectors at the present time. However, advances in semiconductor crystal growth and purification techniques for narrow gap materials such as InSb, InAs, and HgCdTe may provide extrinsic photoconductive detectors which can operate at lower frequencies, perhaps down to 200 GHz.

C. InSb Hot Electron Video Photoconductor

A second mechanism which leads to millimeter and submillimeter photoconductivity involves the mobility change of electrons already in the conduction band upon the absorption of radiation. This effect is generally known by the term hot (or free) electron photoconductivity and has been widely used to provide a sensitive millimeter wave detector, predominantly in InSb. The effect is quite general and has also been observed in Ge [58] and GaAs [56].

Because of their high mobility in high purity semiconductors, electrons in the conduction band are essentially uncoupled from the lattice at liquid helium temperatures and interact predominantly by (Rutherford) scattering from the ionized impurity centers. The cross section for Rutherford scattering is proportional to $1/E^2$ where E is the kinetic energy of the electron. This strong dependence on E produces hot electron photoconductivity because when the electron absorbs radiation by free carrier absorption, its scattering cross section decreases; hence, the mobility increases and one observes a corresponding drop in resistivity across the sample. In contrast to ordinary photoconductive processes where the absorption of radiation allows a carrier to make the transition from a bound state to a high mobility state, the hot electron response increases with increasing wavelength since the cross section for free carrier absorption is

$$\sigma_{\text{free carrier}} = \frac{ne^2}{m^* \left[1 + (\omega\tau)^2\right]} = \frac{\sigma_o}{1 + (\omega\tau)^2}$$

where n is the carrier concentration and τ is the collision time. In InSb the peak responsivity occurs near 1 mm and falls off as $1/\omega^2$ in the submillimeter range.

The InSb hot electron photoconductor is also called the Rollin detector after the individual who suggested its use [59]. Its capabilities were first demonstrated by Kinch and Rollin [60], and it has been widely applied to high sensitivity millimeter and submillimeter measurements where conditions allow

the use of liquid helium. The relative spectral responsivity of the Rollin detector is shown in Figure 14. The NEP at the responsivity peak (in the region between 1 and 2 mm) is approximately 1×10^{-12} W/(Hz)$^{1/2}$, although Vystavkin et al., claim to have measured an NEP of 2×10^{-13} W/(Hz)$^{1/2}$ for this detector by carefully optimizing the detector geometry and the receiving chamber [61].

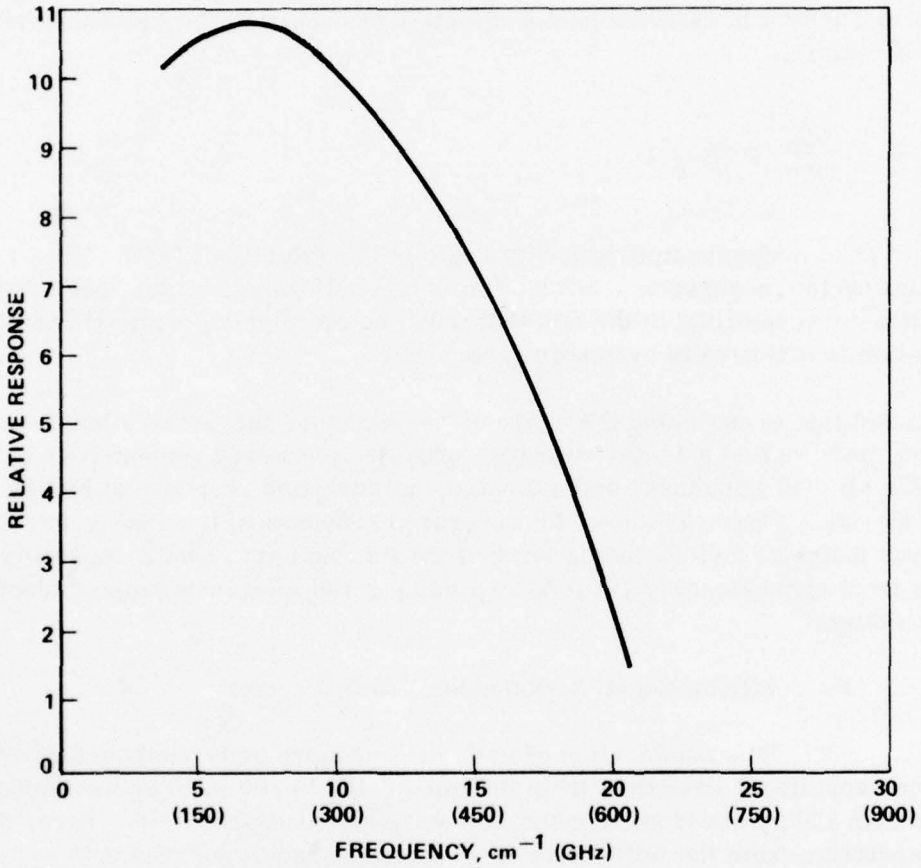

Figure 14. Spectral response of the InSb millimeter wave detector. NEP at peak of response curve is approximately 1×10^{-11} W/(Hz)$^{1/2}$. This can be reduced to 1×10^{-12} W/(Hz)$^{1/2}$ by the use of a cooled step-up transformer or by the application of a dc magnetic field in the range of 4 to 8 kilogauss [63].

D. InSb Cyclotron Resonance Video Detector

The application of a magnetic field to the Rollin detector extends its usefulness into the submillimeter and far-infrared. Free carrier absorption is replaced by cyclotron resonance absorption between adjacent Landau levels in the presence of a dc magnetic field, and just at the frequencies where $\sigma_{\text{free carrier}}$ becomes small, $\sigma_{\text{cyclotron resonance}}$ becomes large and sharply defined in terms of wavelength response. The peak cyclotron resonance absorption (and corresponding photoconductivity) occurs at the Landau level energy separation

$$\Delta E = \frac{\hbar eB}{m^* c} \equiv \hbar\omega_c$$

where B is the magnetic field intensity and c is the velocity of light. The maximum cyclotron resonance absorption is one half the maximum free carrier absorption corresponding to the fact that only one circularly polarized component of radiation is effective in cyclotron resonance.

In addition to extending the range of the detector, the use of a magnetic field with InSb, called a Putley detector, provides increased responsivity at low fields ($B < 10$ kilogauss) and a tunable, narrow band response at higher fields [60-63]. Figure 15 shows the measured response of the Putley detector at various magnetic fields, indicating that the tunable narrow band capability extends from approximately 150 μ to 20 μ using a 100 kilogauss superconducting magnet system.

E. Silicon Negative Donor Ion Video Detector

The combination of InSb and GaAs provides photoconductive detection capabilities extending from the millimeter to 100 μ. For wavelengths shorter than 120 μ, doped germanium detectors are available [64]. Thus, the entire spectrum from the millimeter to 10 μ and beyond is covered with photoconductive detectors. However, the capabilities of mid-infrared detectors (e.g., detectors at 10.6 μ) are superior to those in the millimeter and submillimeter in terms of speed, quantum efficiency, and responsivity.

Speed of response is a particularly serious problem. The response time of the InSb detector is approximately 0.4 msec and, therefore, it cannot provide the bandwidth required for many applications. Recently, Norton [65,66]

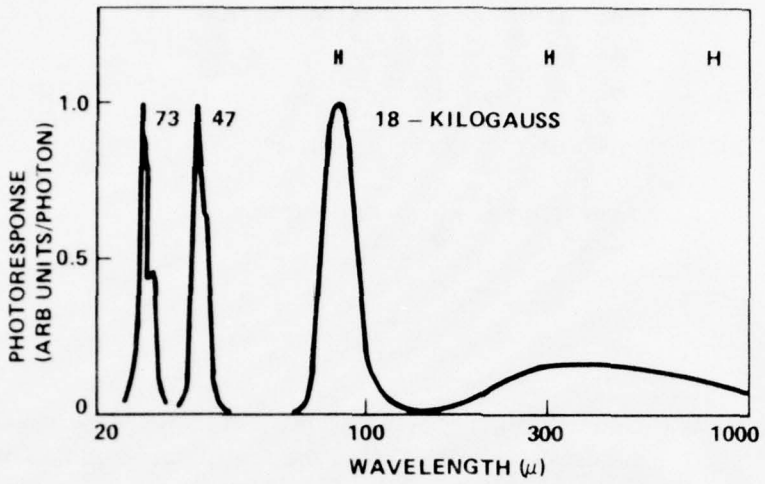

Figure 15. Photoresponse per photon of the InSb Putley detector in arbitrary units plotted against wavelength. The curves have been normalized. Magnetic field strength and spectrometer resolution are indicated [62].

has reported the development of a submillimeter detector which is claimed to have a nanosecond response time and a quantum efficiency of 1 to 5%. The mechanism of photoconductivity is believed to result from the ionization of an electron (weakly) bound to a neutral donor, i.e., ionization from negative donor ions. Relatively heavily doped ($N_D \approx 1 \times 10^{16}$ cm^{-3}), uncompensated n-type silicon is used. In silicon, the ionization energy for neutral donors is rather large, approximately 500 cm^{-1}. To supply electrons which can bind to neutral donors, denoted as D_o sites, unfiltered room temperature background radiation is allowed to illuminate the detector and neutral donors are thereby ionized. Recombination can then occur to either ionized donors, denoted as D^+ sites, or D_o sites, with recombination rates R^+ and R^o, respectively. These processes are illustrated in Figure 16. By operating the detector at high bias levels (approximately 50 V/cm), a reduced recombination rate to D^+ sites is obtained due to the high velocity of electrons ($R^+ \sim 1/E^2$), and electron lifetimes are dominated by capture at D^o centers. Norton [65] estimates that the steady-state concentration of negative donor ions, denoted as D^- sites, is approximately 1×10^{13} cm^{-3}.

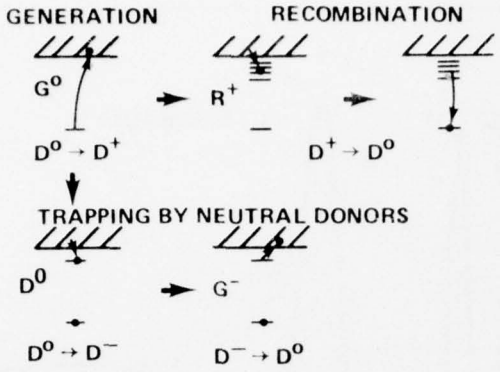

Figure 16. Generation, recombination, and trapping by neutral donor mechanisms are illustrated for the effect each has on the charge state of the donor impurity. The transition made by the electron is shown in each case [65].

The spectral response of the silicon negative donor ion is shown in Figure 17. At the peak of the responsivity curve, near 50 cm^{-1}, the NEP is estimated to be 1×10^{-11} $W/(Hz)^{1/2}$, and it is claimed that heterodyne receiver NEP's of between 1×10^{-19} W/Hz and 5×10^{-19} W/Hz can be obtained with sufficient LO power, which he estimates to be in the range of 50 mW.

Perhaps the most important aspect of the work on the silicon negative donor ion is that it represents the first new photoconductive detector developed for the submillimeter region in a number of years, and the novel concept of using states other than simply hydrogenic impurities to generate a submillimeter photoconductive response suggests a number of variations which could lead to comparable performance in the millimeter. For example, negative donor ion states in germanium should have a lower binding energy than those in silicon, which should push the responsivity curve (Figure 17) to lower frequencies.

There are a number of advantages which bulk photoconductive detectors have over junction devices: (1) relatively large size which allows sufficient coupling of the radiation with conventional optical techniques, (2) ease of fabrication, (3) reproducibility and ruggedness, (4) relative insensitivity to noise and vibration, and (5) inability to be destroyed by improper biasing and turn-on procedures. Therefore, it would be highly desirable to have sensitive, high speed ($\tau \lesssim 5$ nsec) photoconductors capable of operating between 100 and 600 GHz. Such detectors do not exist at the present time; InSb is reasonably sensitive but has a limited bandwidth capability ($\lesssim 2$ MHz). New concepts with

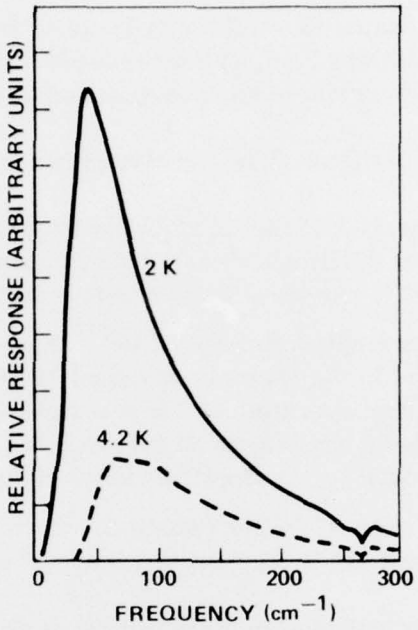

Figure 17. Spectral response of the phosphorous-doped silicon detector is shown at constant far-infrared power for two temperatures [66].

well-characterized semiconductors (such as the silicon negative donor ion) and improved crystal growth techniques of new semiconductor compounds should provide detectors with the required characteristics.

Nevertheless, in spite of the advantages listed for photoconductors, it is unlikely that these detectors, which operate at or below liquid helium temperature, can compete with room temperature junction devices for millimeter wave ($\nu \lesssim 300$ GHz) radar system applications. At frequencies below 300 GHz, state-of-the-art Schottky-barrier diode superheterodyne receiver systems now have sensitivities that are approximately one order of magnitude above the thermal background limit and are continuing to improve. Thus, millimeter wave photoconductors provide, at best, a factor of 10 improvement in signal-to-noise ratio, and this gain is probably insufficient to compensate for the formidable problems of field operation at liquid helium temperature. The same relative numbers and argument apply to video detection at frequencies below 300 GHz.

At submillimeter frequencies between 300 and 600 GHz, the present performance of room temperature junction devices falls rapidly, and the relative advantage of photoconductors is two to three orders of magnitude.

Whether this difference, which is sufficiently large to require a serious consideration of the trade-offs involved, can be reduced with further improvements in junction receiver design remains an open question at the present time.

F. InSb Superheterodyne Receiver System

The potential of the InSb hot electron detector as the mixing element in high sensitivity millimeter wave superheterodyne receivers was noted by Putley in 1966 [1]. Assuming the receiver would be limited by amplifier noise, Putley estimated an NEP of 10^{-18} W/Hz. The capabilities of the detector were realized in the systems designed by Phillips and Jefferts [24,25] in 1973 and 1974 for operation at 115 and 230 GHz, respectively. By using a room temperature IF amplifier (20 kHz to 2 MHz) with eight parallel FET's, they obtained a much lower amplifier noise figure and achieved an overall system NEP of 8×10^{-21} W/Hz (Table 2) which is only a factor of 2 above the fundamental limit set by background thermal noise.

The InSb detector is mounted in a waveguide as shown in Figure 18 and is backed by a tuning reflector. One of the advantages of the InSb mixer is the much lower local oscillator power requirements (10^{-6} W), relative to the Schottky-barrier diode (10^{-2} W), for optimum performance. As a result, a relatively inefficient Schottky-barrier diode doubler, driven by a 115 GHz klystron, provides sufficient local oscillator power for the InSb mixer at 230 GHz. In addition, this receiver should be capable of comparable operation at frequencies as high as 1000 GHz, which is well beyond the frequency capability of present low noise diode mixer systems. A major disadvantage of the system, other than the cryogenic requirements, is that the relatively slow response time of the detector limits the bandwidth to approximately 2 MHz. Nevertheless, the receiver has been very successful in radio astronomy applications. For example, four new interstellar lines were observed in the 200 GHz range, three from CO at 219, 220, and 230 GHz and one from DCN at 217 GHz [25].

In addition to its near ideal NEP and capability of operating equally well over the entire spectral range of interest of this report, the InSb receiver demonstrates the great potential for bulk photoconductors. The major problem that remains is to develop a fast ($\tau \lesssim 5$ nsec) sensitive photoconductor for this region of the spectrum.

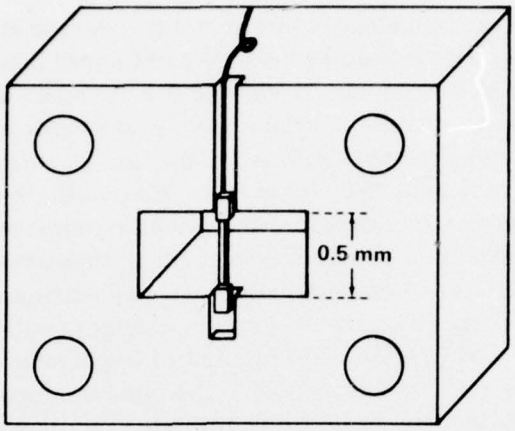

Figure 18. The bulk InSb mixer of Phillips and Jefferts. The semiconductor is shown placed in the RG-137 waveguide. The active region of the bolometer is etched to dimensions of approximately $0.5 \times 1.0 \times 0.1$ mm [25].

VII. RECOMMENDATIONS

The application of millimeter and submillimeter (100 to 600 GHz) wave radar systems to surface-to-surface tracking and missile guidance is at present impacted by the limited availability of sensitive and rugged room temperature superheterodyne receivers, although such receivers, utilizing GaAs Schottky-barrier diodes, have been successfully demonstrated in laboratory environments at frequencies up to 325 GHz. The availability situation grows progressively worse as one moves to higher frequencies, and systems operating above 140 GHz are obtainable on special order only, with delivery times extending to one year and longer. Army support is strongly recommended here to speed up the conversion of scientific realizability into commercial availability. This program should include support for (1) high frequency Schottky diode development, including a critical evaluation of the relative performance of GaAs versus silicon Schottky's operating in the range between 100 and 350 GHz, (2) support for the development of local oscillator sources in this frequency range, particularly stable solid-state oscillators, and (3) support for promising new coupling concepts such as quasi-optical couplers and planar diode arrays which can bypass the increasingly large waveguide losses occurring at these frequencies. Considering the present scientific state-of-the-art, a reasonable but stringent 5 year goal of this program might be, for example, to make sensitive and rugged superheterodyne receiver systems available at all the atmospheric windows in the millimeter (i.e., at 94, 140, 220, and 340 GHz) with a noise figure of less than 7 dB (single sideband) at all frequencies.

The direct detection capabilities of Schottky-barrier diodes in the millimeter has been largely overlooked because the principal applications until now, such as millimeter wave astronomy, required the seven to nine orders of magnitude improvement in sensitivity available from superheterodyne detection. For certain missile guidance applications (e.g., the missile receiver in a beam-rider system), the direct detection sensitivity of Schottky's may be adequate and, if so, would provide a compact and inexpensive solution to a critical problem. Army support for a research program in this area is recommended. Among the problems that need consideration are (1) optimum coupling techniques for video detection, (2) noise spectrum characteristics of millimeter wave Schottky diodes, and (3) the development of appropriate video amplifiers. A related problem that requires attention is the performance of Schottky's in an environment similar to that on an in-flight missile. Planar Schottky's, which are inherently more rugged, may be important for this application.

High speed photoconductors and Josephson junctions are alternatives to Schottky-barrier diodes as detectors in superheterodyne and video receivers. However, both types of devices require liquid helium temperature for operation in the millimeter and submillimeter region, and their sensitivity advantage relative to Schottky's is diminishing with time. In addition to the cryogenic burden, both the photoconductors and Josephson junctions suffer additional problems which have been detailed in this report, and some attention should be given to their resolution.

REFERENCES

1. Putley, E. H., "The Use of an InSb Detector as a Mixer at 1 mm," Proc. IEEE, vol. 54, 1966, pp. 1096-1098.

2. Arams, F. R., Infrared to Millimeter Wavelength Detectors, Artech House, Dedham, Massachusetts, 1973.

3. Dickens, I. E., "Low Conversion Loss Millimeter Wave Mixers," IEEE G-MTT Int. Microwave Symp. Proc., June 1973, pp. 66-68.

4. Leedy, H. M., "Advanced Millimeter Wave Mixer Diodes, GaAs and Silicon, and a Broadband Low-Noise Mixer," Proc. Conf. High Frequency Generation and Amplification, Cornell University, Ithaca, New York, August 17-19, 1971.

5. Fetterman, H. R., Clifton, B. J., Tannenwald, P. E., and Parker, C. D., "Submillimeter Detection and Mixing Using Schottky Diodes," Appl. Phys. Lett., vol. 24, 1974, pp. 70-72.

6. Fetterman, H. R., Clifton, B. J., Tannenwald, P. E., Parker, C. D., and Penfield, Hays, "Submillimeter Heterodyne Detection and Harmonic Mixing Using Schottky Diodes," Proc. First Int. Conf. on Submillimeter Waves and Their Applications, Atlanta, Georgia, 1974. (Published in IEEE MTT Trans., Part I, vol. MTT-22, December 1974, pp. 1013-1015.)

7. Jassby, D. L., Cohn, D. R., Lax, B., and Halverson, W., "Tokamak Diagnostics with the 496-um CH_3F Laser," Nucl. Fusion, vol. 14, 1974, pp. 745-747.

8. Kruse, Paul W., "A System Enabling the Army to See Through Inclement Weather," Army Scientific Advisory Panel Report, June 1974.

9. Hodges, D. T. and McColl, M., "Extension of the Schottky-Barrier Detector to 70 Microns (4.3 THz) Using Submicron Dimensional Contacts," Appl. Phys. Lett., vol. 30, 1977, pp. 5-7.

10. McColl, M. and Hodges, D. T., "Submillimeter-Wave Detection with Submicron-Size Schottky-Barrier Diodes," IEEE MTT Trans., vol. MTT-25, 1977, pp. 463-467.

11. Clifton, B. J., "Schottky-Barrier Diodes for Submillimeter Heterodyne Detection," Proc. of Second International Conf. on Submillimeter Waves and Their Applications, Supplement, San Juan, Puerto Rico, December, 1976, pp. SII-S15. (IEEE Cat. No. 76 CH 1152-8 MTT.)

12. Bernues, F., Kuno, H. J., and Crandell, P. A., "GaAs or Si: What Makes a Better Mixer Diode?," Microwaves, March 1976, pp. 46-55.

13. Wrixon, G. T., "Low-Noise Diodes and Mixers for the 1-2 mm Wavelength Region," IEEE MTT Trans., vol. MTT-22, 1974, pp. 1159-1165.

14. Kerr, A. R., Mattauch, R. J., and Grange, J. A., "A New Mixer Design for 140-220 GHz," IEEE MTT Trans., vol. MTT-25, May, 1977, pp. 399-401.

15. Schneider, M. V. and Wrixon, G. T., "Development and Testing of a Receiver at 230 GHz," IEEE MTT Symposium Digest, 1974, pp. 120-122.

16. Goldsmith, P. F. and Plambeck, R. L., "A 230 GHz Radiometer System Employing a Second Harmonic Mixer," IEEE MTT Trans., vol. MTT-24, November 1976, pp. 859-861.

17. Cohn, M., Wentworth, F. L., and Wiltse, J. C., "High-Sensitivity 100- to 300-Gc Radiometers," Proc. IEEE, vol. 51, 1963, pp. 1227-1232.

18. Chang, S. Y., "Radiometric Measurement of Atmospheric Absorption at 600 Gc/s," Proc. IEEE, vol. 54, 1966, pp. 459-461.

19. Gustinicic, J. J., "A Quasi-Optical Radiometer," Proc. Second International Conf. on Submillimeter Waves and Their Applications, San Juan, Puerto Rico, December 1976, pp. 106-107. (IEEE Cat. No. 76 CH 1152-8 MTT.)

20. Kraemer, E., Kurpis, G., Taub, J., and Grayzel, A., "Quasioptical Circuits Relating to Frequency Multipliers," Proc. Symposium on Submillimeter Waves, New York, 1970, pp. 615-629. (Published by The Polytechnic Press of the Polytechnic Institute of Brooklyn.)

21. Tannenwald, P. E., Far Infrared and Submillimeter Technology, Research Proposal Submitted to Army Research Office, MIT Lincoln Laboratory, 1976. (Also see K. Minzuno, R. Kuwahara and S. Ono, "Submillimeter Detection Using a Schottky Diode with a Long-Wire Antenna," Appl. Phys. Lett., vol. 26, 1975, pp. 605-607.)

22. Snell, W. W. Jr. and Schneider, M. V., "Millimeter-Wave Thin-Film Downconverters," IEEE MTT Trans., vol. MTT-24, November, 1976, pp. 805-807.

23. Edrich, J., "Results, Potentials and Limitations of Josephson Mixer Receivers at MM and Long Submillimeter Wavelengths," Proc. Second International Conf. on Submillimeter Waves and Their Application, San Juan, Puerto Rico, December 1976, pp. 181-182. (Also, see Microwaves, May, 1977, pp. 14.)

24. Phillips, T. G. and Jefferts, K. B., "A Low Temperature Bolometer Heterodyne Receiver for Millimeter Wave Astronomy," Rev. Sci. Instrum., vol. 44, 1973, pp. 1009-1014.

25. Phillips, T. G. and Jefferts, K. B., "Millimeter-Wave Receivers and Their Applications in Radio Astronomy," IEEE MTT Trans., Part II, vol. MTT-22, December, 1974, pp. 1290-1292.

26. McColl, M. and Millea, M. F., "Schottky-Barriers on InSb," Journal of Electronic Materials, vol. 5, 1976, pp. 191-207.

27. McColl, M., Pedersen, R. J., Bottjer, M. F., Millea, M. F., Silver, A. H., Vernon, F. L. Jr., "The Super-Schottky Diode Microwave Mixer," Appl. Phys. Lett., vol. 28, 1976, pp. 159-162.

28. Hadni, A., "Present Status of the Applications of Pyroelectricity to the Detection of Far Infrared Radiation," Proc. First International Conf. on Submillimeter Waves and Their Application, Atlanta, Georgia, 1974, pp. 1016-1018.

29. Hadni, A., "Thermal Infrared Detectors," Proc. Symposium on Submillimeter Waves, New York, 1970, pp. 251-266.

30. Putley, E. H., "Pyroelectric Detectors," Proc. Symposium on Submillimeter Waves, New York, 1970, pp. 267-280.

31. Norton, P., Slusher, R. E., and Sturge, M. D., "Heterodyne Detection in the Far Infrared Using Shallow Impurity States in Silicon," Proc. Second International Conf. on Submillimeter Waves and Their Application, pp. 187-188.

32. Hocker, L. O., Sokoloff, D. R., Daneu, V., Szoke, A., and Javan, A., "Frequency Mixing in the Infrared and Far Infrared Using a Metal-to-Metal Point Contact Diode," Appl. Phys. Lett., vol. 12, 1968, pp. 401-402.

33. Green, S. I., Coleman, P. D., and Baird, J. R., "The MOM Electric Tunneling Detector," Proc. Symposium on Submillimeter Waves, New York, 1970, pp. 369-389.

34. Kerr, A. R., "Low-Noise Room-Temperature and Cryogenic Mixers for 80-120 GHz," IEEE MTT Trans., vol. MTT-23, 1975, pp. 781-787.

35. Cohen, L. D., Nussbaum, S., Kraemer, E., Calviello, J., and Taub, J., "Varactor Frequency Doublers and Triplers for the 200 to 300 GHz Range," IEEE MTT Symposium Digest, 1975, pp. 274-275.

36. Cohn, M., Degenford, J. E., and Newman, B. A., "Harmonic Mixing With an Antiparallel Diode Pair," IEEE MTT Trans., vol. MTT-23, 1975, pp. 667-673.

37. Schneider, M. V., "Harmonically Pumped Stripline Down-Converter," IEEE MTT Trans., vol. MTT-23, 1975, pp. 271-275.

38. McMaster, T. F., Schneider, M. V., and Snell, W. W. Jr., "Millimeter-Wave Downconverter With Subharmonic Pump," IEEE S-MTT Int. Microwave Symp., Digest of Technical Papers, 1976, pp. 185-187.

39. Henry, P. S., Glance, B. S., and Schneider, M. V., "Local-Oscillator Noise Cancellation in the Subharmonically Pumped Down-Converter," IEEE MTT Trans., vol. MTT-24, 1976, pp. 254-257.

40. Elder, H. E., and Glinski, V. J., Microwave Semiconductor Devices and Their Circuit Applications, edited by H. A. Watson, McGraw-Hill, New York, 1969, p. 381.

41. Davidheiser, R., "Is There a Josephson Junction in Your Future?," Microwaves, March, 1977, pp. 50-55.

42. Batt, R. J. and Harris, D. J., "Submillimeter Waves, A Survey of the State-of-the-Art," The Radio and Electronic Engineer, vol. 46, 1976, pp. 379-392.

43. Bauer, R. J., Cohn, M., Cotton, J. M., Jr., and Packard, R. F., "Millimeter Wave Semiconductor Diode Detectors, Mixers, and Frequency Multipliers," Proc. IEEE, vol. 54, 1966, pp. 595-605.

44. Murphy, R. A., Bozler, C. O., Parker, C. D., Fetterman, H. R., Tannenwald, P. E., Clifton, B. J., Donnelly, J. P., and Lindley, W. T., "Submillimeter Heterodyne Detection with Planar GaAs Schottky-Barrier Diodes," IEEE MTT Trans., vol. MTT-25, pp. 494-495, 1977.

45. Josephson, B. D., "Possible New Effects in Superconducting Tunnelling," Phys. Letters., vol. 1, 1962, pp. 251-253.

46. Richards, P. L., Auracher, F., and Van Duzer, T., "Millimeter and Submillimeter Wave Detection and Mixing with Superconducting Weak Links," Proc. IEEE, vol. 61, 1973, pp. 36-45.

47. Blaney, T. G., "Applications of the Josephson Effects in the Millimetre and Submillimetre Wavelength Regions," The Radio and Electronic Engineer, vol. 42, 1972, pp. 303-308.

48. Grimes, C. C., Richards, P. L., and Shapiro, S., "Josephson Effect Far Infrared Detector," J. Appl. Phys., vol. 39, 1968, pp. 3905-3915.

49. Taur, Y., Classen, J. H., and Richards, P. L., "Josephson Junctions As Heterodyne Detectors," Proc. First International Conf. on Submillimeter Waves and Their Application, Atlanta, Georgia, 1974, pp. 1005-1009.

50. Blaney, T. G., "Effect of Bias Voltage on the Frequency Response of Point Contact Josephson Radiation Detectors," Phys. Lett., A., vol. 37, 1971, pp. 19-20.

51. Taur, Y., and Richards, P. L., "Parametric Amplification and Oscillation at 36 GHz Using a Point-Contact Josephson Junction," J. Appl. Phys., vol. 48, 1977, pp. 1321-1326.

52. Ulrich, B. T. and Levinsen, M. T., "First Evidence for 1-mm Wavelength Parametric Amplification in a Josephson Junction Microwave Source," Appl. Phys. Lett., vol. 26, 1975, pp. 131-133.

53. Elsley, R. K. and Sievers, A. J., "Tunable Far Infrared Radiation from Josephson Junctions," Revue de Physique Appliquee, vol. 9, 1974, p. 295.

54. Kanter, H., "Josephson Junction Mixer Using an External Local Oscillator," Revue de Physique Appliquee, vol. 9, 1974, pp. 255-262.

55. Weinreb, S. and Kerr, A. R., "Cryogenic Cooling of Mixers for Millimeter and Centimeter Wavelengths," IEEE J. Solid-State Circuits (Special Issue on Microwave Integrated Circuits), vol. SC-8, 1973, pp. 58-63.

56. Stillman, G. E., Wolfe, C. M., Melingailis, I., Parker, C. D., Tannenwald, P. E., and Dimmock, J. O., "Far-Infrared Photoconductivity in High-Purity Epitaxial GaAs," Appl. Phys. Lett., vol. 13, 1968, pp 83-84.

57. Stillman, C. E., Wolfe, C. M., and Dimmock, J. O., "Detection and Generation of Far Infrared Radiation in High Purity Epitaxial GaAs," Proc. Symposium on Submillimeter Waves, New York, 1970, pp. 345-359.

58. Kaplan, R., "A Method for the Observation of Cyclotron Resonance at Millimeter Wavelengths," Solid State Comm., vol. 3, 1965, pp. 35-38.

59. Rollin, B. V., "Detection of Millimeter and Submillimeter Wave Radiation by Free Carrier Absorption in a Semiconductor," Proc. Phys. Soc., London, vol. 77, 1961, pp. 1102-1103.

60. Kinch, M. A. and Rollin, B. V., "Detection of Millimetre and Submillimetre Wave Radiation by Free Carrier Absorption in a Semiconductor," Brit. J. Appl. Phys., vol. 14, 1963, pp. 672-676.

61. Vystavkin, A. N., Gubankov, V. N., Listvin, V. N., and Migulin, V. V., "Investigation, Development, and Application of 0.1-2.0 mm Receivers with n-InSb Detectors," Proc. Symposium on Submillimeter Waves, pp. 321-329.

62. Putley, E. H., "Impurity Photoconductivity in N-Type InSb," Proc. Phys. Soc., vol. 76, London, 1960, pp. 802-805.

63. Putley, E. H., "Impurity Photoconductivity in N-Type InSb," J. Phys. Chem. Solids, vol. 22, 1961, pp. 241-247.

64. Brown, M. A. C. S. and Kimmitt, M. F., "Far-Infrared Resonant Photoconductivity in InSb," Infrared Physics, vol. 5, 1965, pp. 93-97.

65. Putley, E. H., "Indium Antimonide Submillimeter Photoconductive Detectors," Applied Optics, vol. 4, 1965, pp. 649-656.

66. Moore, W. J. and Shenker, H., "A High-Detectivity Gallium-Doped Germanium Detector for the 40-120 Micron Region," Infrared Physics, vol. 5, 1965, pp. 99-106.

67. Norton, P., "Photoconductivity From Shallow Negative Donor Ions in Silicon: A New Far Infrared Detector," J. Appl. Phys., vol. 47, 1976, pp. 308-320.

68. Norton, P., Slusher, R. E., and Sturge, M. D., "Far Infrared Detection Using Photoconductivity of Negative Donor Ion States in Silicon," Appl. Phys. Lett., vol. 30, 1977, pp. 446-448.

DISTRIBUTION

	No. of Copies
Defense Documentation Center	
Attn: DDC-TGA	12
Cameron Station	
Alexandria, Virginia 22314	
Commander	
US Army Research Office	
Attn: Dr. R. Lontz	2
P.O. Box 12211	
Research Triangle Park	
North Carolina 27709	
US Army Research and Standardization Group (Europe)	
Attn: DRXSN-E-RX	
Dr. Alfred K. Nedoluha	2
Box 65	
FPO New York 90510	
US Army Materiel Development and Readiness Command	
Attn: Dr. Gordon Bushy	1
Dr. James Bender	1
Dr. Edward Sedlak	1
5001 Eisenhower Avenue	
Alexandria, Virginia 22333	
Headquarters	
Hq	
DA (DAMA-ARZ)	2
Washington, D.C. 20310	
Director of Defense Research and Engineering	
Engineering Technology	
Attn: Mr. L. Weisberg	2
Washington, D.C. 20301	
Director	
Defense Advanced Research Projects Agency	
1400 Wilson Boulevard	
Arlington, Virginia 22209	1
Commander	
US Army Aviation Systems Command	
12th and Spruce Streets	
St. Louis, Missouri 63166	1
Director	
US Army Air Mobility Research and Development Laboratory	
Ames Research Center	
Moffett Field, California 94035	1
Commander	
US Army Electronics Command	
Attn: DRSEL-TL-I, Dr. Jacobs	1
DRSEL-CT, Dr. R. Buser	1
Fort Monmouth, New Jersey 07703	
Director	
US Army Night Vision Laboratory	
Attn: John Johnson	1
Fort Belvoir, Virginia 22060	

	No. of Copies
Director	
Atmospheric Sciences Laboratory	
US Army Electronics Command	
White Sands Missile Range	
New Mexico 88002	1
Director	
US Army Ballistic Research Laboratories	
Attn: Ken Richer	1
Aberdeen Proving Ground, Maryland 21005	
Commander	
US Army Combined Arms Combat Development Activity	
Fort Leavenworth, Kansas 66027	1
Commander	
US Army Frankford Arsenal	
Philadelphia, Pennsylvania 19137	1
Commander	
US Army Picatinny Arsenal	
Dover, New Jersey 07801	1
Commander	
US Army Tank Automotive Development Command	
Attn: DRDTA-RWL	1
Warren, Michigan 48090	
Commander	
US Army Mobility Equipment Research and Development Command	1
Fort Belvoir, Virginia 22060	
Commander	
US Army Harry Diamond Laboratories	
2800 Powder Mill Road	
Attn: Dr. Stan Kulpa	1
Adelphi, Maryland 20783	
Commander	
US Army Armament Command	
Rock Island, Illinois 61202	1
Commander	
US Army Foreign Science and Technology Center	
Federal Office Building	
220 7th Street, NE	
Charlottesville, Virginia 22901	1
Commander	
US Army Training and Doctrine Command	
Fort Monroe, Virginia 23351	1
Director	
Ballistic Missile Defense Advanced Technology Center	
Attn: ATC-D	1
ATC-O	1
ATC-R	1
ATC-T	1
P.O. Box 1500	
Huntsville, Alabama 35807	
Commander	
US Naval Air Systems Command	
Washington, D.C. 20360	1

	No. of Copies
Chief of Naval Research Department of the Navy Washington, D.C. 20360	1
Commander US Naval Air Development Center Attn: Radar Division Warminster, Pennsylvania 18974	1
Commander US Naval Electronics Lab Center San Diego, California 92152	1
Commander US Naval Surface Weapons Center Dahlgran, Virginia 22448	1
Commander US Naval Weapons Center Attn: Mr. Robert Moore China Lake, California 93555	1
Director Naval Research Laboratory Attn: Code 5300, Radar Division Dr. Skolnik Code 5370, Radar Geophysics Br Code 5460, Electromagnetic Prop Br Washington, D.C. 20390	1 1 1
Commander Rome Air Development Center Attn: R. McM llan, OCSA James Wasielewski, IRRC Griffiss Air Force Base, New York 13440	1 1
Commander US Air Force, AFOSR/NP Attn: LT COL Gordon Wepfer Bolling Air Force Base Washington, D.C. 20332	1
Commander US Air Force Avionics Laboratory Attn: D. Rees CPT James D. Pryce, AFAL/WE Dr. B. L. Sowers, AFAL/RWI Wright Patterson Air Force Base, Ohio 45433	1 1 1
Commander (AFGL) Hanscom Air Force Base, Massachusetts 01731	1
Commander AFATL/LMT Eglin Air Force Base, Florida 32544	1
Dr. D. T. Hodges, Jr. The Aerospace Corporation 2350 East El Segundo Boulevard Los Angeles, California 90009	1
Commander Center for Naval Analyses Attn: Document Control 1401 Wilson Boulevard Arlington, Virginia 22209	1
Hughes Aircraft Company Missile System Group Attn: Dr. J. A. Glassman Canoga Park, California 91304	1
Goodyear Aerospace Corporation Arizona Division Attn: Mr. Fred Wilcox Mr. P. W. Murray Litchfield Park, Arizona 85340	1 1
Honeywell, Inc. Systems and Research Division Attn: Dr. Paul Kruse Minneapolis, Minnesota 55413	1
Raytheon Company Attn: A. V. Jelalian 528 Boston Post Road Sudbury, Massachusetts 01776	1
Dr. Richard Temkin MIT National Magnet Lab Albany St. Cambridge, Massachusetts 02132	1
Dr. D. R. Cohn MIT National Magnet Lab Albany St. Cambridge, Massachusetts 02132	1
Georgia Institute of Technology Engineering Experiment Station Attn: James Gallager 347 Ferst Drive Atlanta, Georgia 30332	1
The Rand Corporation Attn: Dr. S. J. Dudzinsky, Jr. 1700 Main Street Santa Monica, California 90406	2
Hughes Research Laboratory Attn: Mr. Smith John F. Heney J. M. Baird 3011 Malibu Canyon Road Malibu, California 90265	1 1 1
Environmental Research Institute of Michigan Radar and Optics Division Attn: Dr. A. Kozma Dr. C. C. Aleksoff P.O. Box 618 Ann Arbor, Michigan 41807	1 1
Dr. J. G. Castle Physics Department University of Alabama 4701 University Drive, NW Huntsville, Alabama 35807	1
Science and Technology Division Institute of Defense Analysis Attn: Dr. Vincent J. Corcoran 400 Army-Navy Drive Arlington, Virginia 22202	1

	No. of Copies
Director Calspan Corporation Attn: R. Kell P.O. Box 235 Buffalo, New York 14221	1
California Institute of Technology Attn: Dr. N. George 1201 E. California Boulevard Pasadena, California 91109	1
Optical Science Consultants Attn: Dr. D. L. Fried P.O. Box 388 Yorba Linda, California 92686	1
ADTC/SRCE Attn: D. Dingus Eglin Air Force Base, Florida 32542	1
Office of Naval Research/ Code 221 Attn: D. C. Lewis 800 N. Quincy Street Arlington, Virginia 22217	1
Pacific Missile Test Center Code 3253 Attn: Charles Phillips Point Mugu, California 93042	1
The Aerospace Corporation Attn: C. M. Randall Box 92957 Los Angeles, California 90009	1
Dr. P. E. Tannenwald Division 8 MIT Lincoln Laboratory Lexington, Massachusetts 02173	1
Dr. H. R. Fetterman Division 8 MIT Lincoln Laboratory Lexington, Massachusetts 02173	1
AFCL (OPI) Attn: John Selby Hanscom Air Force Base Bedford, Massachusetts 01731	1
Pacific-Sierra Research Corporation Alan R. Shapiro Vice President 1456 Cloverfield Boulevard Santa Monica, California 90404	1
Commander Code 3173 Naval Weapons Center Attn: Dr. Alexis Shlanta China Lake, California 93555	1
Naval Surface Weapons Center Attn: Mary Tobin WR42 White Oak, Maryland 20910	1

	No. of Copies
Environmental Research Institute of Michigan Infrared and Optics Division Attn: Anthony J. LaRocca Robert L. Spellicy P.O. Box 618 Ann Arbor, Michigan 48107	1 1
ElectroScience Laboratory Department of Electrical Engineering The Ohio State University Attn: Dr. Ronald K. Long 1320 Kinnear Road, Columbus, Ohio 43212	1
Atmospheric Sciences Laboratory US Army Electronics Command Attn: Dr. Mishri L. Vatsia White Sands Missile Range New Mexico 88002	1
DRSMI-LP, Mr. Voigt	1
DRDMI-X, Dr. McDaniel	1
-T, Dr. Kobler	1
Mr. Dobbins	25
-TE, Mr. Lindberg	1
Mr. Todd	1
Mr. Pittman	1
-TEO, Mr. Ducote	1
Dr. Emmons	20
Mr. Farmer	1
Mr. Grass	1
Dr. Carruth	1
Mr. Mitchell	1
Mr. Hodgens	1
Dr. Waldman	25
-TER, Dr. Loomis	1
Mr. Spaulding	1
-TEG, Mr. Green	1
-TEM, Mr. Harraway	1
-CBG, Mr. Evans	1
Mr. Dooley	1
-TR, Dr. Hartman	1
Dr. Guenther	1
Dr. Gamble	1
-TBD	3
-TI (Reference Set)	1
(Reference Copy)	1